WIND-TUNNEL MODEL STUDY OF DOWNWASH FROM STACKS AT MAUI ELECTRIC COMPANY POWER PLANT, KAHULUI, HAWAII

by

J. E. Cermak* and S. K. Nayak**

Prepared under contract to
Stearns-Roger Incorporated
700 South Ash, Denver
Colorado 80222

Fluid Dynamics and Diffusion Laboratory
Department of Civil Engineering
College of Engineering
Colorado State University
Fort Collins, Colorado

March 1973

CER72-73JEC-SKN28

*Professor-in-Charge, Fluid Mechanics Program

**Research Engineer

ABSTRACT

Tests were conducted in the meteorological wind-tunnel using 1:200 scale model to determine the distribution of gas concentration resulting from gaseous plumes released from four stacks associated with Maui Electric Company Power-Plant at Kahului Hawaii. The tests were conducted over a model power-plant including all significant structures in the vicinity. Data obtained included photographs and color motion pictures of smoke-plume trajectories and plots of contaminant concentration down wind of the power-plant at ground-level sampling positions. The effects of wind direction and stack height on ground-level concentrations are established. Evaluation of test results revealed that an increase of stack height from 30.48 m to 60.96 m will reduce the maximum ground-level concentrations by a factor of three to five depending upon the wind direction. Location of stacks upwind of the power-plant structures was found to show distinct improvement of plume characteristics.

TABLE OF CONTENTS

LIST OF TABLES

LIST OF FIGURES

LIST OF FIGURES - Continued

LIST OF SYMBOLS

Symbol	Definition	Dimension
A	Cross sectional area of stack	L^2
d	Diameter of stack	L
E	Eckert number	
F_e	Equivalent vertical momentum	ML^2/T^2
F_m	Vertical momentum	ML^2/T^2
g	Gravitational acceleration	L/T^2
Δh	Plume rise	L
h	Stack height	L
H	Effective stack height	L
K	Concentration coefficient	
L	Characteristic length	L
n	Exponent of power law of velocity profile	
Q	Total source strength	m/T
q	Source strength of each stack exhaust	m/T
Pr	Prandtl number	
Re	Reynolds number $\frac{uL}{\nu}$	
Ri	Richardson number $(\frac{\Delta T_o}{T_o} \frac{L}{u^2})/g$	
Ro	Rossby number $\frac{U}{L\Omega}$	
T	Temperature	
ΔT	Temperature difference $(T - T_\infty)$	
U_∞	Free-stream velocity	L/T
u	Local velocity of air stream (horizontal)	L/T
V	Exit velocity of exhaust at stack height	L/T
x,y,z	General coordinate system - downwind, lateral and upwards as shown in Fig. 1	L

LIST OF SYMBOLS - continued

Symbol	Definition	Dimension
XYZ	General coordinate system - downwind, lateral and upwards as shown in Fig. 1	
c	Local concentration	m/L^3
T	Sampling time	T
o	Azimuth angle of upwind direction measured from magnetic north	
γ	Ratio of stack exhaust velocity to local velocity	
δ	Boundary-layer thickness	L
ν	Kinematic viscosity	L^2/T
ρ	Mass density	m/L^3
Ω	Angular velocity of earth	1/T

Subscripts:

cmax	Condition at maximum ground-level concentration
e	Equivalent
h	Condition at stack height h
m	Model
max	Maximum
o	Initial condition
p	prototype
s	Stack
1,2,3,4,	Stack numbers as shown in Fig.
∞	Condition at free stream

I. INTRODUCTION

A wind tunnel study of the Maui Electric Company Power-Plant was motivated by the desire to determine the minimum height of stacks which will eliminate downwash and reduce the concentration of sulfur dioxide at ground-level such that it can meet the Hawaii ambient air-quality standards. The field measurements carried out by Beckner (1) have revealed that sulfur dioxide from the power-plant stack exhaust contribute to the local environment pollution to the extent that the air quality does not meet the required local air-quality standards.

The power-plant is located in Wailuku-Kahului, near the sea shore. Its peculiar location is such that the ambient wind carries the stack exhaust over the city. The wind direction for about 90% of the time varies within the limits of ± 15° from the northeast at a typical wind velocity with gusts at 20 kn. A typical measurement by Beckner (1) indicated that the maximum daily average value of sulfur dioxide concentration was approximately eleven times greater than that permitted by the Hawaiian air-quality standards.

It has been a traditional design criterion to release the exhaust gases through the top of tall stacks located near the power-plant, where the stack height is at least two and one-half times taller than the nearby buildings. Calculations of peak and mean ground-level concentrations of these gases are then based on some semi-empirical model which relates the release rate from an elevated point source to the concentration at some point down-wind. Models have been suggested by Sutton (2), Pasquill (3), Roberts (4), and Cramer (5). These models require the assumption of plane homogeneous atmospheric turbulence and constant mean lateral and mean vertical velocities. These assumptions are satisfied for a point release over a flat undisturbed terrain.

In addition, considerable effort has been made to determine the effect of vertical stack velocity and gas buoyancy on the effective stack release height. Briggs (6), Carson and Moses (7) have reviewed over 15 plume rise formulas constructed to calculate the effective stack height for conditions where there are no effects from local terrain or buildings. They concluded that no available plume-rise equations can be expected to accurately predict short-term plume rise.

Often it is desirable due to aesthetics, cost and maintenance of good public relations to utilize a shorter stack or vent connected directly to the power-plant. In these cases the plume dispersion is sufficiently modified by the presence of local building structures or ground topography that the only approach available for determination of concentration field is by means of a wind-tunnel model study (8, 9, 10).

A number of wind-tunnel studies have investigated the effects of variation in geometry of a single building or plume entrainment and dispersion (11, 12, 13, 14). These studies have permitted the specification of pertinent scaling criteria for model studies of plume excursions near buildings. There exists in the literature descriptions of a variety of different model studies on diffusion near reactor and industrial plants (9, 10, 15, 16, 17, 18, 19, 20). These studies are significant in that their results have been essentially confirmed by either direct prototype measurements or absence of gases or particulates where the study predicted this would be the result. Martin (19) compared his wind-tunnel concentration data about a model of the Ford Nuclear Reactor at the University of Michigan with prototype measurements.

Munn and Cole (21) have made concentration measurements on a power-station complex at the National Research Establishment, Ottawa, Canada, to confirm the general entrainment criteria suggested by the model studies of Davies and Moore (16). The agreement of the pollution concentration measurements with the field values were usually satisfactory.

The objective of this study is to reduce the sulfur-dioxide concentration at ground-level to an acceptable level by releasing the exhaust at a greater elevation of minimum height such that the effect of downwash due to the local buildings and other structures will be eliminated. To accomplish this objective a model investigation in which stack height is varied systematically was designed.

A systematic wind-tunnel study was planned which consisted of a two-stage program of measurements on a geometrically similar model of power-plant structures and down-wind buildings of 1:200 scale. In the first stage, downwash characteristics as a function of stack height and wind direction was observed through flow visualization by discharging smoke from the four stacks. Motion pictures were made of down-wind plumes to provide permanent record (Appendix D). The second stage consisted in measuring actual tracer gas concentrations at ground-level for a down-wind distance of 3000 meters. These measurements provide direct evidence that the effect of downwash is eliminated for a particular stack height, permit evaluation of the reduction in ground-level concentration for additional stack height increases and provide information on the magnitude and location of maximum ground-level concentrations.

II. SIMULATION OF ATMOSPHERIC MOTION

The use of a wind-tunnel for model tests of gas diffusion by the atmosphere is based upon the concept that nondimensional concentration coefficients will be the same at contiguous points in the model and the prototype and will not be a function of the length scale ratio. Concentration coefficients will only be independent of scale if the wind-tunnel boundary layer is made similar to the atmospheric boundary layer by satisfying certain similarity criteria. These criteria are obtained by inspectional analysis of physical statements for conservation of mass, momentum and energy. Detailed discussions have geen given by Halitsky (11), Martin (19) and Cermak (22). Basically the model laws may be divided into requirements for geometric, dynamic, thermic and kinematic similarity. In addition, similarity of up-wind flow characteristics and ground boundary conditions must be achieved.

For the Maui Electric Company Power-Plant study, geometric similarity is satisfied by an undistorted model of length ratio 1:200. This scale was chosen to facilitate ease of measurements, provide a boundary layer equivalent to 300 m for the atmosphere and minimize wind tunnel blockage. (The ratio of projected area to the area of the wind tunnel cross section should not exceed 5%. The model of Maui Electric Company Power-Plant at a scale of 1:200 produced a blockage of 1.9%.)

Dynamic similarity is achieved in a strict sense if a Reynolds number $(\frac{UL}{\gamma})$, a Richardson number $[\frac{(\Delta T_o/T_o)}{g}(L/u^2)]$ and a Rossby number $(\frac{U}{L\Omega})$ for the model is equal to its counterpart for the atmosphere. The Reynolds number for the model exceeded 10^4 which is the lower critical value established by Golden (9) for flow patterns to become independent of Reynolds number. The minimum Reynolds number encountered in the present study was 15,000 based on a building model width of 0.3 m and minimum velocity of 0.915 m/sec. Strong atmospheric winds were found to give maximum downwash. For these winds thermal stratification is of little significance. Therefore, all plumes were modeled in isothermal boundary layer or for zero Richardson number. The model Rossby number cannot be made equal to the atmospheric value. However, over the short distances considered (up to 3000 m), the Coriolis acceleration has little influence upon the flow. Accordingly, the standard practice is to relax the requirement of equal Rossby numbers (10, 22). Correlation tests of flow about the Rock of Gibraltar (23), flow over Pt. Arguelo, California (24), and flow over San Nicolas Island, California (20) may be cited as examples of large Reynolds number flows which have been modeled successfully in a wind tunnel.

Thermic similarity requires equality of model and prototype Prandtl numbers and Eckert numbers. However, because of the isothermal modeled flows, these equalities were not necessary.

Kinematic similarity requires similarity of mean velocity and turbulence characteristics of the approach flow with corresponding quantities in the atmospheric boundary layer. These requirements are automatically satisfied through use of the long wind-tunnel test section and appropriate surface roughness (22). An additional kinematic requirement is associated with the stack-gas jet. The ratio of stack-gas exit speed to wind speed at stack exit should be equal for model and prototype for exhaust gas at air ambient density. However, actual stack-gas temperatures were above that of the ambient air. Therefore, to simulate the effect of stack-gas buoyancy without changing density of the model stack-gas an increment of exit speed was added to give a plume rise effect equivalent to the buoyancy effect (see Appendix A).

The simulated approach mean-wind conditions were described by an exponent of the velocity distribution power law of $n = 0.16$. This was found to be adequate for an upstream rough sea condition (26). Approach velocity was modified by suitably adjusting the roughness condition upwind of the model such that the measured velocity profile confirmed with the following relation.

$$\frac{U(z)}{U(z_1)} = \left(\frac{z}{z_1}\right)^n$$

where $n = 0.16$.

The need for scaling of the atmospheric mean wind profile was demonstrated by Jensen (14). Substitution of a uniform velocity profile for a logarithmic profile results in a three fold variation in the dimensionless pressure coefficient downstream of a model building. Such variance in the pressure fields indicate a strong effect of the upstream wind profile on the kinematic behavior of the fluid near the building complex. The only tunnel currently capable of generating a turbulent boundary layer thick enough for a 1:200 scale model is the meteorological wind-tunnel at Colorado State University (25). Other investigators have attempted to generate special grids upstream of the test section; however, this technique normally creates nontypical turbulence field which decays rapidly downstream.

Buildings and building complexes produce nonuniform fields of flow which perturb the regular upstream atmospheric wind profiles. Around each building a boundary layer exists, where the velocity is zero at the surface but increases rapidly to a relatively constant value a short distance from the building walls. Outside the boundary layer and downstream there exists a region of low velocities and pressures called the cavity. In this region circulations are such that flow actually reverses direction with respect to the upstream winds. Surrounding the cavity and extending further downstream is a parabolic region called the wake in which the presence of the buildings is still evident in terms of deviation of velocity, turbulence and pressure from conditions found in the upstream atmospheric boundary layer. Lower pressure conditions prevailing in the wake region exert strong influence on the plume in drawing it closer to ground level. The purpose of the present model study has been primarily to establish the minimum stack height that would keep the exhaust plume free from the influence of building wakes. Figure 10 establishes the size characteristics of the wake. A series of pictures shown in Fig. 12 compares the influence of location of stack 3 with respect to the power-plant on the plume characteristics.

III. WIND-TUNNEL AND MEASUREMENT TECHNIQUES

A. Wind-Tunnel

The model study was conducted in the meteorological wind-tunnel of the Fluid Dynamics and Diffusion Laboratory at Colorado State University shown in Fig. 1. The wind-tunnel, specially designed to study atmospheric flow phenomena has a 2 m square and 26 m long test section with an adjustable ceiling to provide a zero pressure gradient over modeled terrain (22, 25). Specially designed roughness floor strips with 3 cm gravel elements are located just upstream from the test section entrance serve to stabilize the flow pattern as well as provide thicker turbulent boundary layer. The test facility permits variation of mean ambient velocity between 0.1 and 37 m/sec. The boundary layer thickness at the downstream portion of the test section can be adjusted between 0.3 and 1.3 m.

B. Model

The model consisted of power-plant, stacks, and auxiliary buildings constructed to a linear scale of 1:200. The basic flat topography was reproduced by fixing the model complex on a large plywood sheet which could be rotated into positions corresponding to different wind directions. The surface roughness length Z_o was typically 1 cm for the prototype and could be satisfactorily modeled by a smooth wind-tunnel floor. The model was built to dimensions taken from reference 1 and Betchel Corporation drawings 5366-C-13-3. Model stacks were made of 6mm (ID) brass tubing and were passed through the wind-tunnel floor so as to facilitate easy variation of stack height. A metered quantity of tracer gas was allowed to flow through each stack to simulate the exit velocity and also account for buoyancy effects due to temperature difference between the stack gas and the ambient atmosphere. The method of correcting exit stack-gas velocity to account for buoyancy effect of hot stack gas is directed in Appendix A. Four model stacks were tested. All the building models were constructed from styrofoam and painted with black latex paint.

C. Flow Visualization Technique

Smoke was used to define plume behavior over the power-plant complex. The smoke was produced by passing humid air over titanium-tetrachloride located in a container outside the wind-tunnel. The smoke (titanium oxide) was transported through tygon tubes to the stack inlets, visible plumes were recorded by means of still pictures (Figs. 10, 12, and 13) and a series of color motion pictures (see Appendix D) which constitute a separate part of the final report. Stack heights were increased until the plume of stack exhaust remained above the building complex. A mean ambient wind speed of 0.915 m/sec was used for all visualization studies. The approach flow velocity distribution is shown in Figs. 8 and 9.

D. Gas Tracer Technique

After the flow in the tunnel was stabilized, a mixture of Kr-85 of predetermined concentration (0.211 μci/cc) was released from model stacks at a required rate (Appendix B). Samples of air were withdrawn from the sample points on the wind-tunnel floor (Figs. 5 and 14) and analyzed. The flow rate of Kr-85 mixture was controlled by a pressure regulator at the supply cylinder outlet and monitored by Fischer and Porter precision flow meters (Appendix C). Source concentration was 0.211 μci/cc of Kr-85, a beta emitter (half life time = 10.3 years). The sampling and detection systems are shown in Figs. 2, 3, 4 and 5 and described in Ref. 27. A sampling grid of 40 sample points was spaced on the wind-tunnel floor (Figs. 5 and 14) at suitable locations to establish the plume axis and locate the points of maximum ground-level concentrations. A reference sample point was located in the free stream, upwind of the model to measure the background concentration in the tunnel. The general arrangement of the sample points for the three directions investigated is shown in Fig. 14.

IV. TEST PROGRAM AND RESULTS

A. Test Program

The test program consisted of two stages. In the first stage a qualitative study of exhaust plume and flow field around the power-plant complex was made by visual observation of smoke trajectories. Plume characteristics from each stack were studied separately by recording smoke plumes on a 16 mm color motion picture which supplements this report (Appendix D). Flow visualization studies were conducted for various stack heights and model stack exhaust flows as detailed in Appendix B. Special visualization studies were conducted on stack 3 to expose the effect of location of the stacks with respect to the power-plant structures along the direction of flow (Fig. 12). Observations were also recorded with all the plumes operating simultaneously and discharging flows as computed in Appendix B. In the second stage of the study the qualitative findings from stage one were confirmed by making quantitative measurements. Concentration measurements were made downwind of stacks by allowing corresponding discharge of Kr-85 and air mixture through each of the stacks. Only the cases with all the stacks operating simultaneously were studied in this stage.

Direction of the approach winds are referred to in terms of azimuth angle from magnetic north. Downwind distances, x , refer to the lengths as measured from stack 4. Unless otherwise noted, the term wind velocity refers to the free stream velocity above the tunnel boundary layer, however, a velocity at any reference height is available by referring to the velocity profiles shown in Fig. 8.

B. Test Results: Visualization

The test results consist primarily of color motion pictures (Appendix D) which supplement this report. The motion pictures depict the characteristics of exhaust plumes from each of the stacks 1, 3 and 4 for their heights varying from 30.48 m to 98.44 m in steps of 7.62 m . The visualization study (Fig. 12) reveals that the cavity-influence behind the power-plant structures on the plumes is pronounced for all cases with stack heights less than 60.96 m . It also reveals that the plumes from stack 1 and 2 contribute heavily to the downwash, whereas, those from stack 3 and 4, by virtue of higher exit gas velocity, remain above the cavity for all cases of stack heights. Downwash from each of the stacks was found to be very severe when stack height was 30.48 m . It was also found that influence of the power-plant structure on the plume was more severe when the stack was located downwind than that when located upwind (Fig. 12). For wind direction 030°N , the downwash is seen to be a minimum, when the wind direction is 045° N or 060° N the downwash effect becomes more severe.

C. Test Results: Concentration Measurements

Since the conventional point-source diffusion equation cannot be used for predicting diffusion near objects which cause the wind to be nonuniform and nonhomogeneous in velocity and turbulence, it is necessary to calculate gaseous concentrations on the basis of experimental data. It is convenient to express the diffusion results in terms of non-dimensional concentration factors independent of model and prototype scale. Halitsky (9) and Martin (19) have discussed the problem in detail. It is suggested that the concentration measurements be transformed to K - isopaths by the formula

$$K = \frac{cuL^2}{Q} \qquad \text{where} \quad \begin{aligned} c &= \text{sample volume concentration} \\ L &= \text{characteristic length} \\ u &= \text{velocity at stack height} \\ Q &= \text{tracer gas release rate} \end{aligned}$$

For the present case L and u remain constant for each case and hence characteristics of K - isopaths can be represented by $\frac{c}{Q}$ - isopaths. The results of the present investigation are represented by $\frac{c}{Q}$ - isopaths.

Concentration measurements were made downwind of stacks at suitable points (Figs. 5 and 14) by passing required quantity (Appendix B) of tracer gas through each of the four stacks simultaneously. Stack heights of 30.48 m, 53.34 m, 60.96 m and 68.58 m were investigated. Concentration measurements were made at ground-level sections 229 m, 394 m, 788 m, 1182 m, 1576 m, and 1970 m from stack 4. Centerline concentration measurements were made from 131 m to 3152 m downwind of stack 4.

Results of the concentration measurements are summarized in Figs. 15 to 23. The effect of stack height on the center line concentration distribution is exposed in Figs. 15, 17 and 19 for approach wind directions 045° N, 060° N and 030° N, respectively. Corresponding concentration distributions at various transverse sections are shown in Figs. 16a to 16d, 18a to 18d, and 20a to 20d respectively. Figure 21 shows the variation of concentration at Maui Meat Company with stack height for the wind direction of 045° N.

In general, it is evident that the concentration of pollutant is reduced by a factor of three to five by increasing the stack height from 30.48 m to 60.96 m depending upon the wind direction.

Figure 22 describes the percentage reduction of maximum ground-level concentration with stack height. Effects of downwash due to the local structures on short stacks (less than 53.34 m) as seen by flow visualization studies is confirmed by the quantitative measurements, represented in this figure, by the significantly higher rate of increase of maximum ground-level concentrations as the stack height is decreased. The effect of wind direction on the maximum concentration distribution illustrated by this figure confirms also that 045° N wind direction produces the highest ground-level concentrations.

Figure 23 represents the variation with stack height the downwind distance where the maximum ground-level concentration occurs, for the three wind directions tested. It appears that the nature in which the point of maximum ground-level concentration shifts in the downwind direction is similar for all the three wind directions tested.

A close examination of ground-level concentration distribution at different sections down-wind of sources (Figs. 16, 18 and 20) for each of the wind directions reveals that the meandering effect of the plume is insignificant.

V. CONCLUSIONS

The investigation was undertaken to determine the dispersion of exhaust gases released from stacks of Maui Electric Company Power-Plant by employing simulation techniques in a wind-tunnel. The primary aim of the study was to determine the optimum height of the stacks which would eliminate downwash and reduce the concentration of sulfur-dioxide to meet the local air quality standards.

On the basis of the experimental measurements reported here, the following conclusions may be made:

1) The influence of local structures on the plume characteristics is severe when the stack height is 30.48 m (present height).

2) A stack height of 60.96 m raises the plumes clear of the influence of local structures. A stack height of 68.58 m should be sufficient to eliminate downwash effect even for power-plant operation at less than capacity loads.

3) Concentration measurements indicate that the pollution at ground-level is reduced by a factor of three to five when the stack height is increased from 30.48 to 60.96 m depending upon the wind direction.

4) Location of stacks on the upwind side of power-plant structures shows a distinct improvement in the plume characteristics.

REFERENCES

1. Beckner, J.L., "Ambient Sulfur Dioxide Surveillance", Kahului, Hawaii, Stearns-Roger Incorporated; Denver, Colorado, Private Communication, September 1972.

2. Sutton, O.G., "The Theoretical Distribution of Airborne Pollution from Factory Chimneys," Quart. J.R. Met. Soc., 73, p. 426, 1947.

3. Pasquill, F., "Atmospheric Diffusion," D. Von Nostand Co., London 1962.

4. Roberts, O.F.T., "The Theoretical Scaling of Smoke in a Turbulent Atmosphere," Proc. Roy. Soc., A104, p. 640.

5. Cramer, H.E., "A Practical Method of Estimating the Disposal of Atmospheric Contaminants," Proc. of 1st Nat. Conf. on Appl. Met., Appl. Met. Soc., C, pp. 33-35, Hartford, Conn., October 1957.

6. Briggs, G.A., "Plume Rise," AEC Critical Review Series, Div. of Tech. Information, 1969.

7. Carson, J.E., and H. Moses, "Validity of Currently Popular Plume Rise Formulas," VSAEC, Met. Information Meeting, Sept. 11-14, 1967, Chalk River, Canada, AECL 2728, pp. 1-15.

8. Moses, H., G. H. Strom and J.E. Carson, "Effect of Meteorological and Engineering Factors on Stack Plume Rise," Nuclear Safety, Vol. 6, No. 1, pp. 1-19, 1966.

9. Halitsky, J., J. Golden, P. Halpern, and P. Wu, "Wind Tunnel Tests of Gas Diffusion From a Leak in a Shell of a Nuclear Power Reactor and Nearby Stacks," Geophys. Sci. Lab. Report No. 63.2, New York University, April 1963.

10. Cermak, J.E., "Laboratory Simulation of the Atmospheric Boundary Layer," AIAA J., Vol. 9, pp. 1746-1754, Sept. 1971.

11. Halitsky, J., "Gas Diffusion Near Buildings," Geophys. Sci. Lab. No. 63.3, New York University, Feb. 1963.

12. Storm, G.H., M. Hackman, and E.J. Kaplin, "Atmospheric Disposal of Industrial Stack Gases Determined by Concentration Measurements in Scale Model Wind-Tunnel Experiments," J. APCA, Vol. 7, 3, pp. 198-204, Nov. 1957.

13. Evans, B.H., "Natural Air Flow Around Buildings," Research Report 59, Texas Eng. Experimental Station, 1957.

14. Jensen, M. and N. Frank, "Model Scale Test in Turbulent Wind," Part I, Danish Tech. Press, Copenhagen 1963.

15. Kalinske, A.A., "Wind-Tunnel Studies of Gas Diffusion in Typical Japanese Urban District," Nat. Def. Res. Council, OSCRD, Informal Report No. 10.3A-48 and 48a, 1945.

16. Davies, P.O.A.L., and P.J. Moore, "Experiments on Behavior of Effluent Emitted from Stacks at or Near Roof Level of Tall Reactor Buildings," Int. J. Air-water Pollution, Vol. 8, pp. 515-533, 1964.

17. Sherlock, R.H. and E.A. Stalker, "The Control of Gases in the Wake of Smoke Stacks," Mech. Engr., Vol. 62, 6, pp. 455-458, June 1940.

18. Hohenleiten, H.L. von, and E. Wolf, "Wind Tunnel Tests to Establish Stack-height for River Side Generating Stations," Trans. ASME, Vol. 64, pp. 671-683, Oct. 1968.

19. Martin, J.E., "The Correlation of Wind Tunnel and Field Measurements of Gas Diffusion Using Kr-85 as Tracer," Ph.D. dissertation, MMPP 272, University of Michigan, June 1968.

20. Meroney, R.N. and J.E. Cermak, "Wind-Tunnel Modeling of Flow and Diffusion over San Nicolas Island, California, U.S. Navy Contract N123(61756)50192A(PMR), Colorado State University report No. CER66-67-RNM-JEC-44, Sept. 1967.

21. Munn, R.E. and A.F.W. Cole, "Turbulence and Diffusion in the Wake of a Building," Atmospheric Environment, Vol. 1, pp. 33-43, 1967.

22. Cermak, J.E. et. al., "Simulation of Atmospheric Motion by Wind Tunnel Flows," Colorado State University report No. CER66-JEC-VAS-EJP-GJB-HC-RNM-SI-17, May 1966.

23. Field, J.H. and R. Warden, "A Survey of Air Current in the Bay of Gibralter," 1929-1930, Airministry Geophys. Mem., No. 59, London 1933.

24. Cermak, J.E., and J. Peterka, "Simulation of Windfields over Point Arguello, California, by Wind-Tunnel Flow over Topographical Model", Final Report U.S. Navy Contract N126(61756)34361A(PMR), Colorado State University Report Number CER65-JEC-JAP64, December 1965.

25. Plate, E.J. and J.E. Cermak, "Micro-Meteorological Wind-Tunnel Facility: Description and Characteristics," Fluid Dynamics and Diffusion Laboratory Report No. CER63-EJP-JEC9, Colorado State Univeristy, 1963.

26. Davenport, A.G., "Gust Loading Factors", Proceedings ASCE, J. Struc. Div., ST3, pp. 11-34, 1967 .

27. Chaudhry, F.H., and R.N. Meroney, "Turbulent Diffusion in a Stably Stratified Shear Layer," U.S.Army Electronic Command Tech. Report C-0423-5, Colorado State University Report Number CER69-70-FHC-RNM12.

APPENDIX

APPENDIX A

Effect of Buoyancy of Stack Exhaust

The present study is an effort to establish the plume characteristics of Maui Electric Company Power-Plant by wind-tunnel simulation techniques. The problem of simulating buoynacy effects of the plume is difficult. Calculations indicate that high temperatures like 1100°F are necessary for model exhaust gas in order to meet this simulation. An alternative method was used to take into account the effect of buoyancy by supplying additional equivalent vertical momentum to the stack exhaust gases.

Examination of several cases of plume rise by Briggs (6) shows that the profile of center line plume with simple jet effect in a uniform flow traces a path given by

$$\Delta h = 2.3\, F_m^{1/3}\, u^{-2/3}\, x^{1/3} \tag{A1}$$

The rise for a buoyant plume in a uniform flow field is described as follows:

$$\Delta h = 2.3\, F_m^{1/3}\, u^{-2/3}\, x^{1/3}\, \left(1 + \frac{Fx}{F_m u}\right)^{1/3} \tag{A2}$$

An equivalent jet effect to represent the buoyant plume can be obtained by matching the plume rise given by Eq. (A1) and (A2) at a suitable distance downwind of the source. In the present study the plume rises are matched at 180 m downwind of stacks where the storage structures are located. Thus,

$$\left(1 + \frac{Fx}{2F_m u}\right) = \frac{F_{me}}{F_m} = \frac{V_{oe}^2}{V_o^2} = \left\{1 + \frac{x}{2V_o}\left(\frac{\rho}{\rho_o} - 1\right)\frac{g}{u_o}\right\} \tag{A3}$$

For an average stack exhaust temperature of 370°F and velocity at stack height, 15.72 m/sec and V_o = 23.6 m/sec and $\frac{V_{oe}}{V_o}$ = 1.5099. Thus, $1.5V_o$ is used as the equivalent stack exhaust velocity that accounts for the effect of buoyancy.

APPENDIX B

Simulation of Stack Exhausts

For the present study stack exhaust was simulated by maintaing the ratio of stack exhaust velocity to the local velocity at the stack top, for the model equal to 1.5 times the prototype value. The effect of buoyancy (as described in Appendix A) was found to produce an effective exhaust velocity of 1.5 times the prototype exhaust velocity.

The following calculations give the details of simulation.

Approach Conditions

a) Wind velocity which gave maximum SO_2 concentration = 20kn

b) Height at which wind velocity was measured in the field = 3 m

c) Approach = Ocean, rough

d) Approximate exponent of power law = 0.16

e) Velocity distribution with height = $\frac{u(z)}{u(z_1)} = (\frac{z}{z_1})^{0.16}$

f) Atmospheric boundary layer for the above condition is assumed to be 490 meters

Details of Simulation

a) Free-stream velocity in the field = 21.8 m/sec

b) Exhaust velocity ratio = $\frac{V}{u(Z)} = \gamma$

c) Size of the model stack 6 mm (ID)

d) Range of stack heights studied = 30.48 m - 91.44 m

e) Scale of the model = 1:200

f) Ambient velocity for flow visualization studies = 0.915 m/sec

g) Ambient velocity for concentration measurements = 1.8 m/sec

h) Stack exit velocity at height $h = \frac{V_p}{u(Z)} \cdot u(h)_m = V$

i) Stack discharge of hot gas = AV = q

j) Equivalent stack discharge of gas at ambient temperature = Q = 1.50 q .

k) Concentration of SO_2 is assumed to be the same for all the stack exhausts

l) Concnetration of tracer gas Kr-85 and air mixture = 0.211 uci/cc

The following tables summarize the results of computations. Table I gives the details of exit velocity ratios. Table II shows the results of calculations for discharges from model stacks for various stack heights for both visualization studies and concentration measurements.

Table I. Exit Velocity Ratios

Stack No.	ΔT oF.	V m/sec	$\frac{V}{u(30.5)}$*	$\frac{V}{u(38.1)}$	$\frac{V}{u(45.72)}$	$\frac{V}{u(53.34)}$	$\frac{V}{u(60.96)}$	$\frac{V}{u(68.58)}$	$\frac{V}{u(91.44)}$
1	270	10.39	0.79	0.76	0.74	0.72	0.71	0.69	0.66
2	305	8.83	0.67	0.65	0.63	0.61	0.60	0.59	0.56
3	300	18.47	1.40	1.36	1.32	1.28	1.26	1.23	1.18
4	315	41.91	3.19	3.08	2.99	2.92	2.85	2.80	2.67

* (z) - meters

Table II. Calculation of Model Stack Discharges for a) flow visualization studies

Stack Height model m	prototype m	velocity model m/sec	Stack 1 V m/sec	q_1 cc/min	Q_1 cc/min	Stack 2 V_2 cc/min m/sec	q_2 cc/min	Q_2 cc/min	Stack 3 V_3 m/sec	q_3 cc/min	Q_3 cc/min	Stack 4 V_4 m/sec	q_4 cc/min	Q_4 cc/min
0.1524	30.48	0.730	0.579	1100	1650	0.491	933	1399	1.024	1946	2919	2.335	4437	6655
0.1905	38.10	0.762	0.579	1100	1650	0.494	938	1408	1.036	1968	2952	2.347	4458	6687
0.2286	45.72	0.792	0.585	1112	1667	0.500	950	1424	1.045	1986	2979	2.368	4498	6748
0.2667	53.34	0.808	0.582	1106	1660	0.494	938	1408	1.033	1964	2946	2.359	4484	6725
0.3048	60.96	0.838	0.594	1130	1694	0.503	955	1434	1.055	2004	3006	2.390	4541	6812
0.3429	68.58	0.853	0.588	1118	1677	0.503	955	1434	1.049	1993	2989	2.39	4541	6812
0.4572	91.44	0.899	0.594	1129	1693	0.503	955	1434	1.061	2015	3022	2.402	4562	6843

Table II. Calculation of Model Stack Discharges for b) concentration measurements

0.1524	30.48	1.323	1.046	1986	2980	0.884	1680	2520	1.853	3.522	5283	4.206	7994	11990
0.2667	53.34	1.448	1.046	1986	2980	0.884	1680	2520	1.853	3.522	5283	4.228	8034	12052
0.3048	60.96	1.494	1.061	2016	3024	0.896	1703	2555	1.881	3.574	5361	4.258	8092	12138
0.3429	68.58	1.524	1.052	1998	2998	0.899	1709	2564	1.875	3.502	5344	4.267	8109	12164

APPENDIX C

Instrumentation and Materials Employed:

Camera	movie:	Bolex 16 mm camera lens
	still:	Speed Graphic Camera 4" x 5"
Film	movie:	Ectachrome - 7242, ASA 125 - Forced developed ASA 500
	still:	Tri-X-Pan-4164 Kodak film
Exposure	movie:	f-1.9, 18 frames per second
	still:	f = 8-11, t = 1/50 sec
Flow meters	1)	Fischer & Porter Co. Precision flow rator No. B4-21-10 float B SVT-45
	2)	Fischer & Porter Co. Precision flow rator No. FP1/4-09-G-G3/4 / 4 / 61
	3)	Fischer & Porter Co. Precision flow rator No. 2F-1/4-20-5/70
Counters	1)	Ultra scaler - model 192A by Nuclear Chicago
	2)	Ortec timer model 482, Scaler model-484 power supply model 446, amplifier model 485 ratemeter model 441

Hot-Wire Anemometer Disa 55D05 Battery Operated constant temperature anemometer.

Hot Wire Pt (80%) Ir (20%) wire, diameter - 0.1 mm, mounted on probe support made at C.S.U.

Traversing Mechanism Made at C.S.U., with remote control, range 0.5 m

Recorder Hewlett and Packard X-Y Recorder Model 7035B

Meter HP Integrating digital voltmeter model 2401C

Pressure Meter MKS Barotran pressure meter type 77 with pressure head type 77 range 0-30 mm Hg

Sampling Panels
1) Made at D.S.U., 25 sample point capacity as shown in figure 4
2) Radioactive gas samplers (figure 3)
   a) Nooo14-68-A-0493-0001-65234
   b) Nooo14-68-A-0493-0001-65227

APPENDIX D

Details of the flow visualization study recorded in the motion pictures are given in the following table:

S. No.	Stack No.	Stack ht. m	Wind direction	Remarks
1	General Introduction			
2	General view from outside tunnel			
3	General view from inside the tunnel			
4	1,2,3,4	30.48	045° N	
5	"	30.48	030° N	
6	"	30.48	060° N	
7	"	53.34	045° N	
8	"	53.34	030° N	
9	"	53.34	060° N	
10	"	60.96	045° N	
11	"	60.96	030° N	
12	"	60.96	060° N	
13	"	68.58	045° N	
14	"	68.58	030° N	
15	"	68.58	060° N	
16	"	91.44	045° N	
17	"	91.44	030° N	
18	"	91.44	060° N	
19	1	30.48	045° N	
20	"	30.48	030° N	
21	"	30.48	060° N	
22	"	53.34	045° N	
23	"	53.34	030° N	
24	"	53.34	060° N	
25	"	60.96	045° N	
26	"	60.96	030° N	
27	"	60.96	060° N	
28	"	68.58	045° N	
29	"	68.58	030° N	
30	"	68.58	060° N	
31	"	91.44	045° N	
32	"	91.44	030° N	
33	"	91.44	060° N	
34	3	30.48	045° N	
35	"	30.48	030° N	
36	3	30.48	060° N	
37	"	53.34	045° N	
38	"	53.34	030° N	
39	"	53.34	060° N	
40	"	60.96	045° N	
41	"	60.96	030° N	
42	"	60.96	060° N	
43	"	68.58	045° N	
44	"	68.58	030° N	
45	"	68.58	060° N	
46	"	91.44	045° N	
47	"	91.44	030° N	
48	"	91.44	060° N	
49	4	30.48	045° N	
50	"	30.48	045° N	
51	"	30.48	060° N	
52	"	53.34	045° N	
53	"	53.34	030° N	
54	"	53.34	060° N	
55	"	60.96	045° N	
56	"	60.96	030° N	
57	"	60.96	060° N	
58	"	68.58	045° N	
59	"	68.58	030° N	
60	"	68.58	060° N	
61	"	91.44	045° N	
62	"	91.44	030° N	
63	"	91.44	060° N	
64	1,2,3,4	68.58	045° N	Far D/S
65	"	60.96	045° N	
66	"	53.34	045° N	
67	"	30.48	045° N	
68	3	68.58	045° N	*

*Down wash behind stack structure at low wind velocities.

Figures

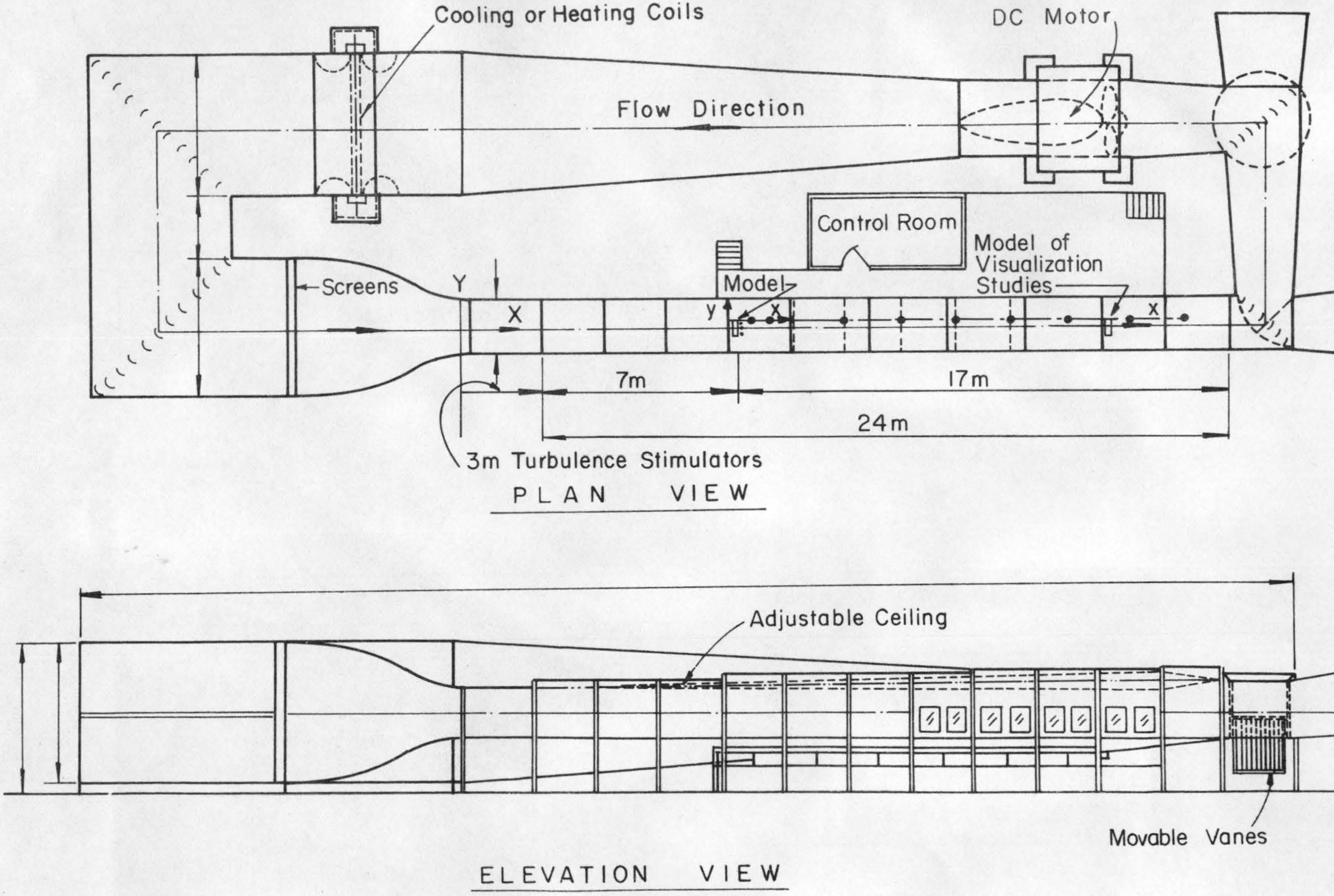

Fig. 1. Army Meteorological Wind Tunnel

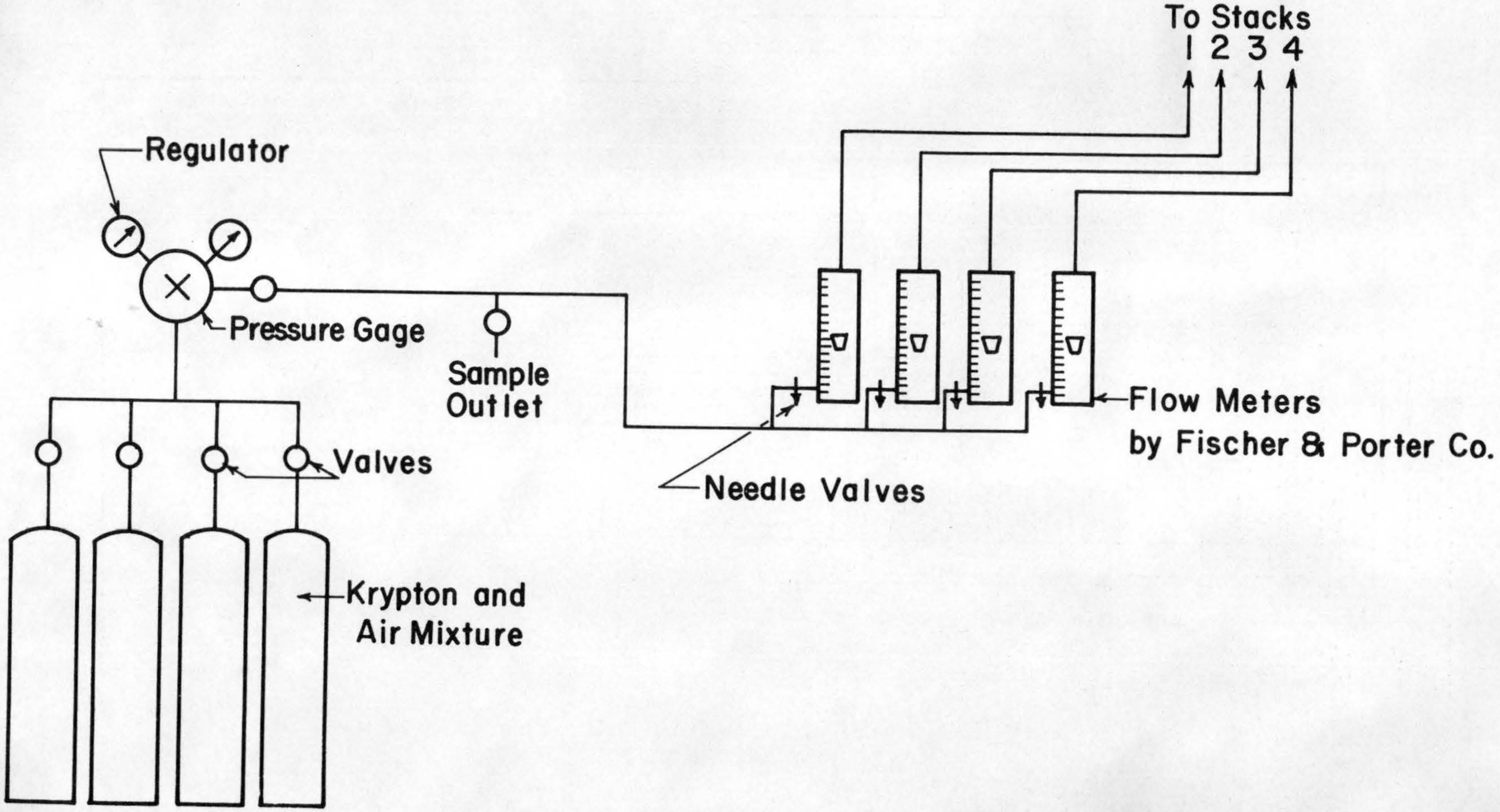

Fig. 2. Stack Gas and Tracer Distribution System

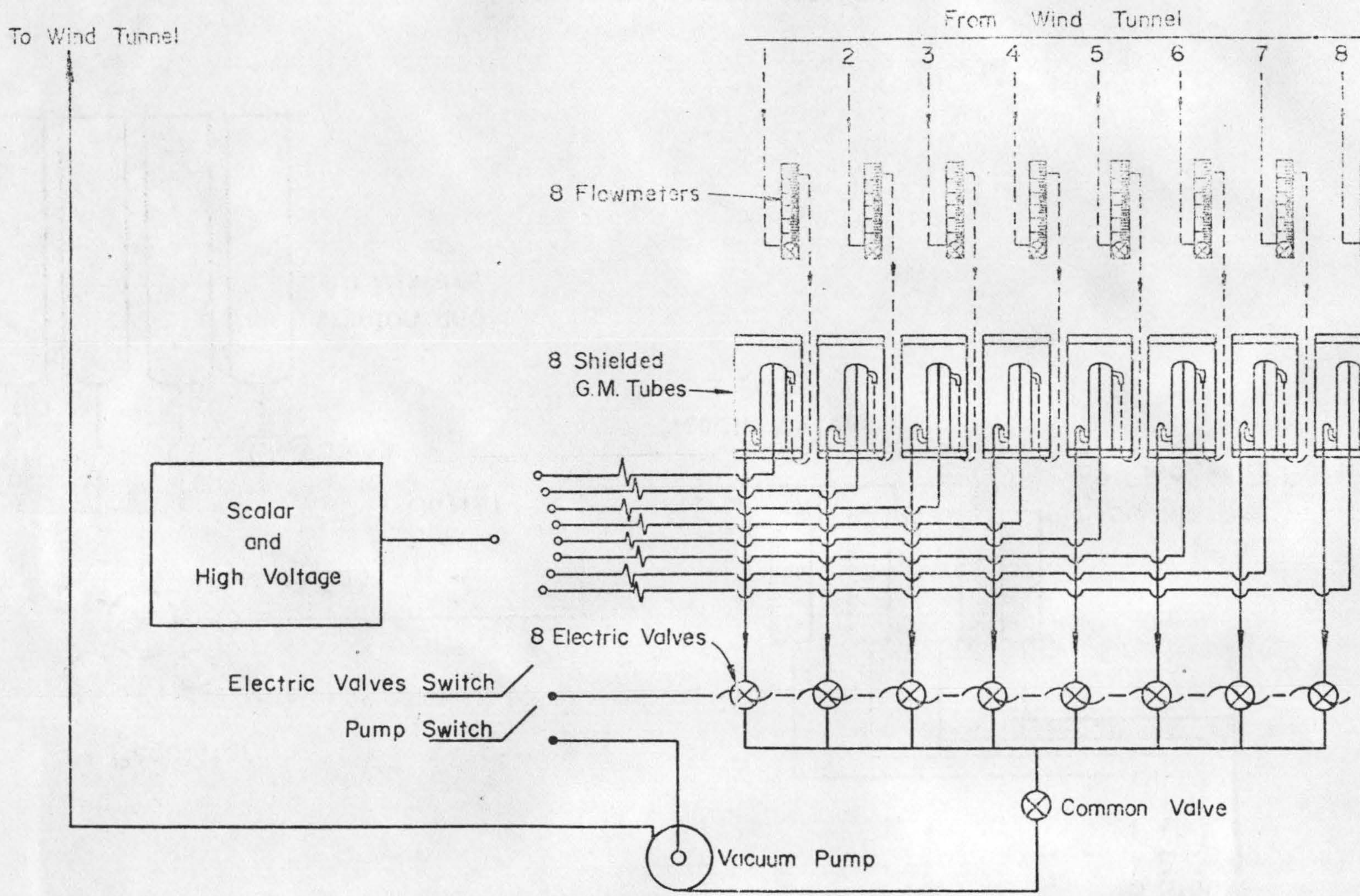

Fig. 3. Detection system 1.

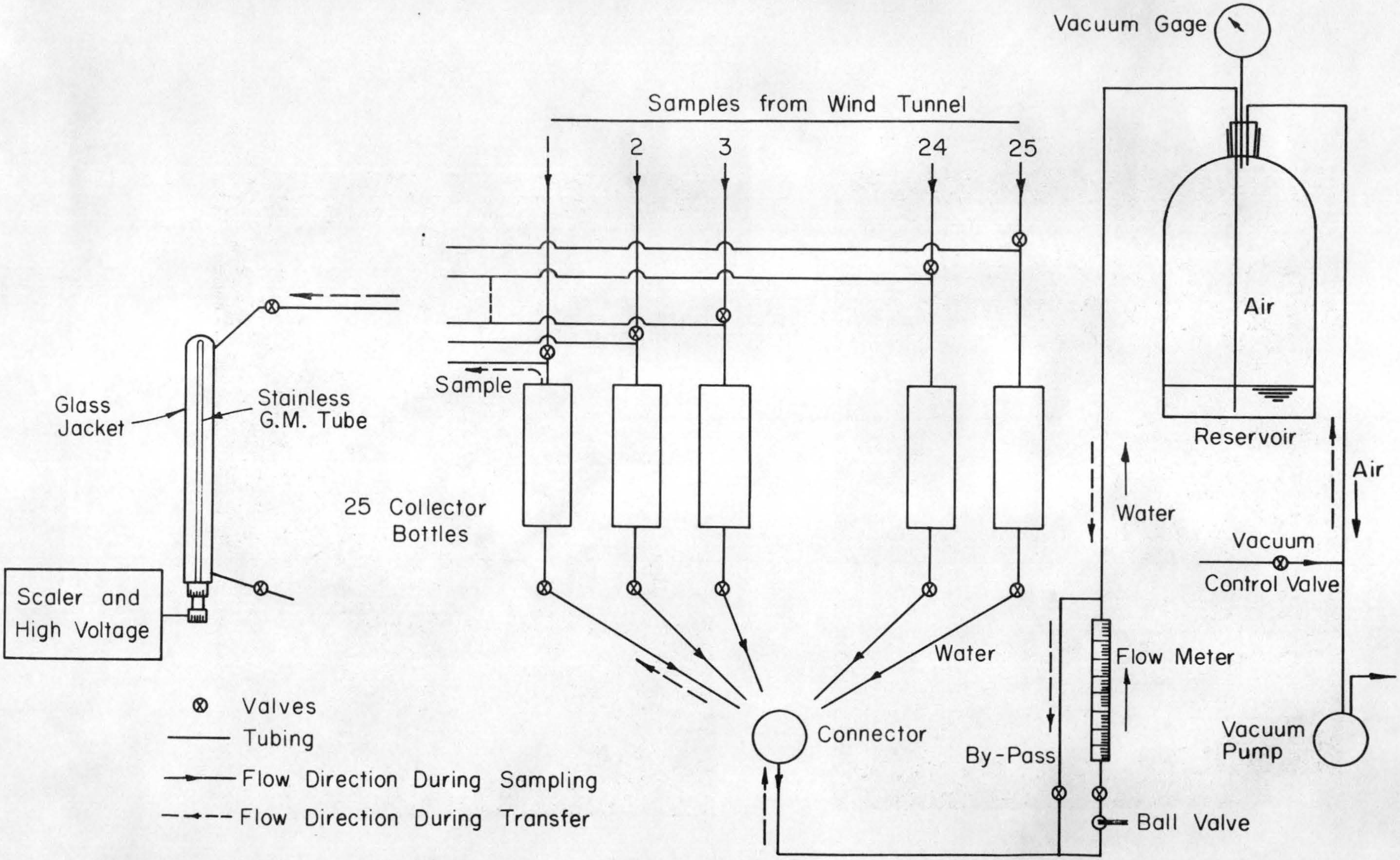

Fig. 4. Tracer-gas sampling and analysis system (16).

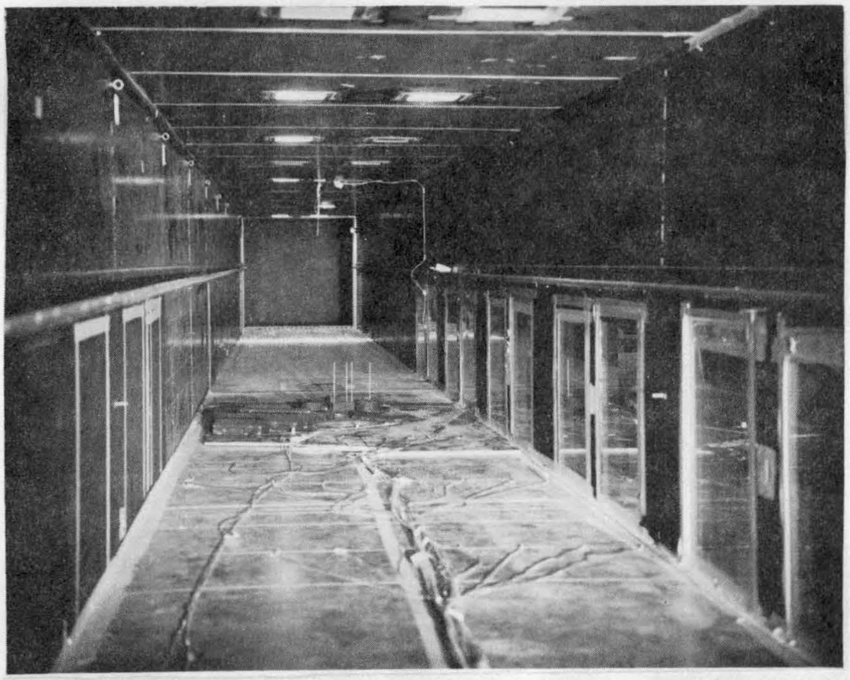

Fig. 5 Distribution of sampling points in the test facility

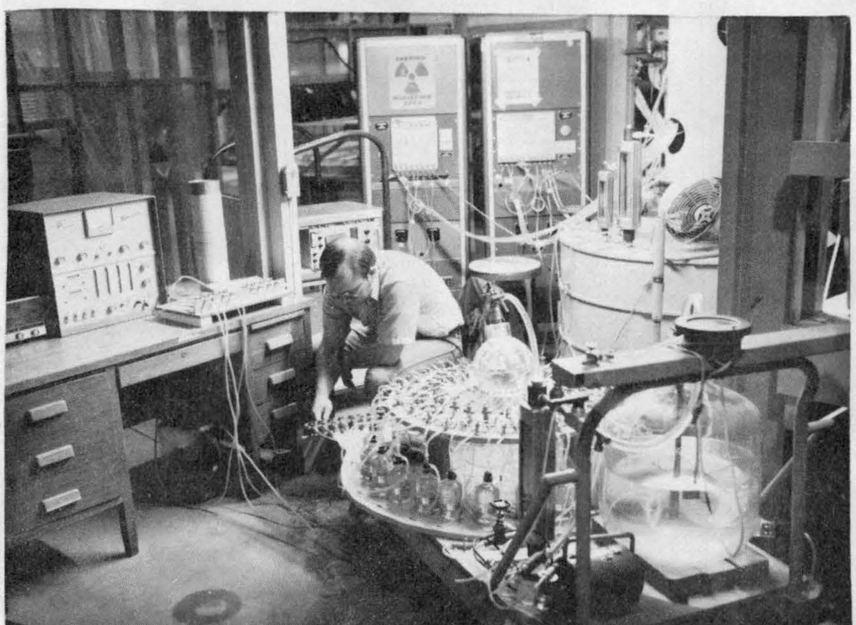

Fig. 6 A view of detection and sampling system

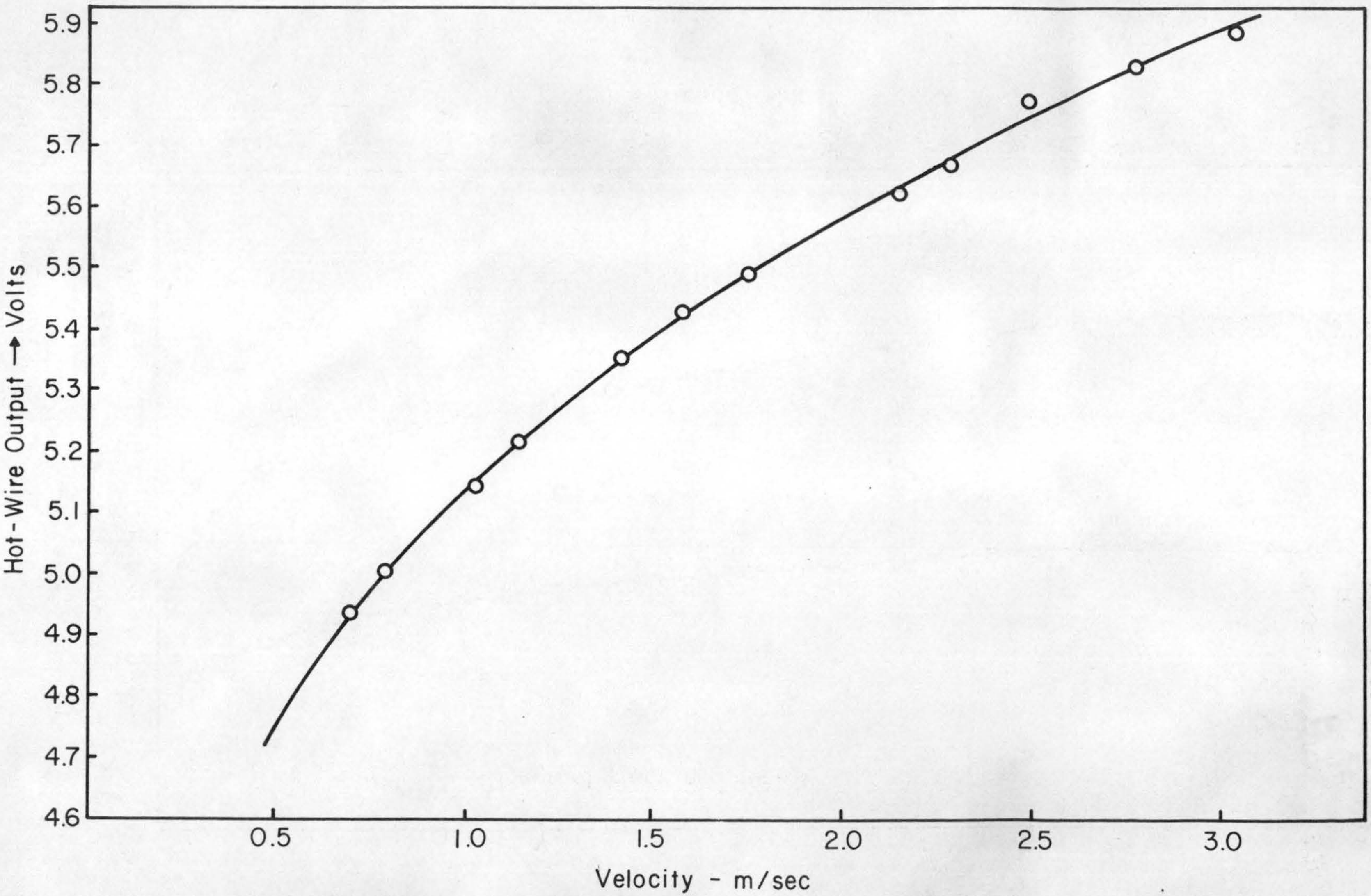

Fig. 7. CALIBRATION OF HOTWIRE: Pt. 80% Ir. 20%, D=0.01mm L=12mm R_C=42.7Ω, γ=1.288, T_W-T_∞=650°F.

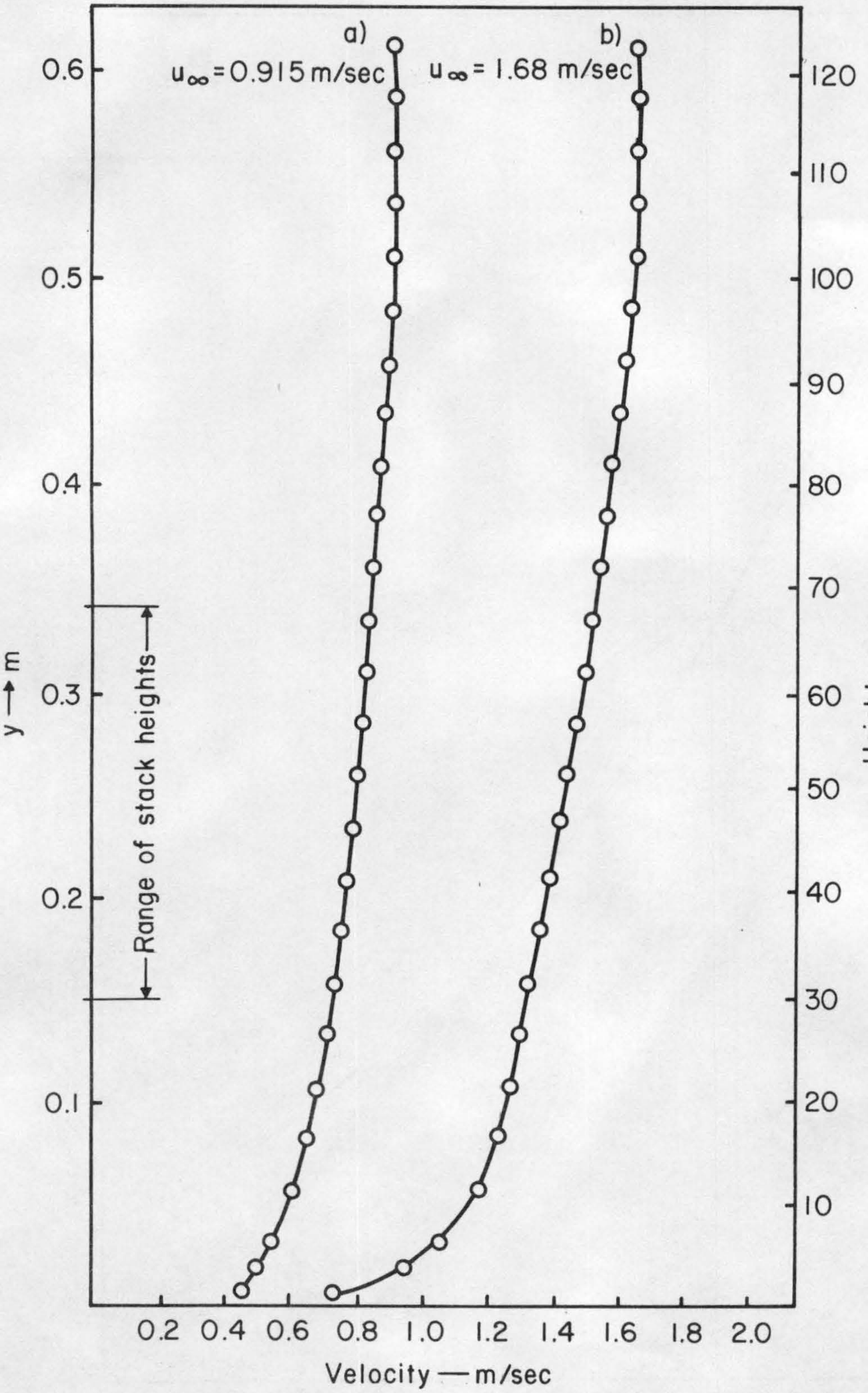

Fig. 8. Velocity profiles for a) Plume visualization
b) Concentration Distribution measurements

at χ = 9m. γ = 0 .

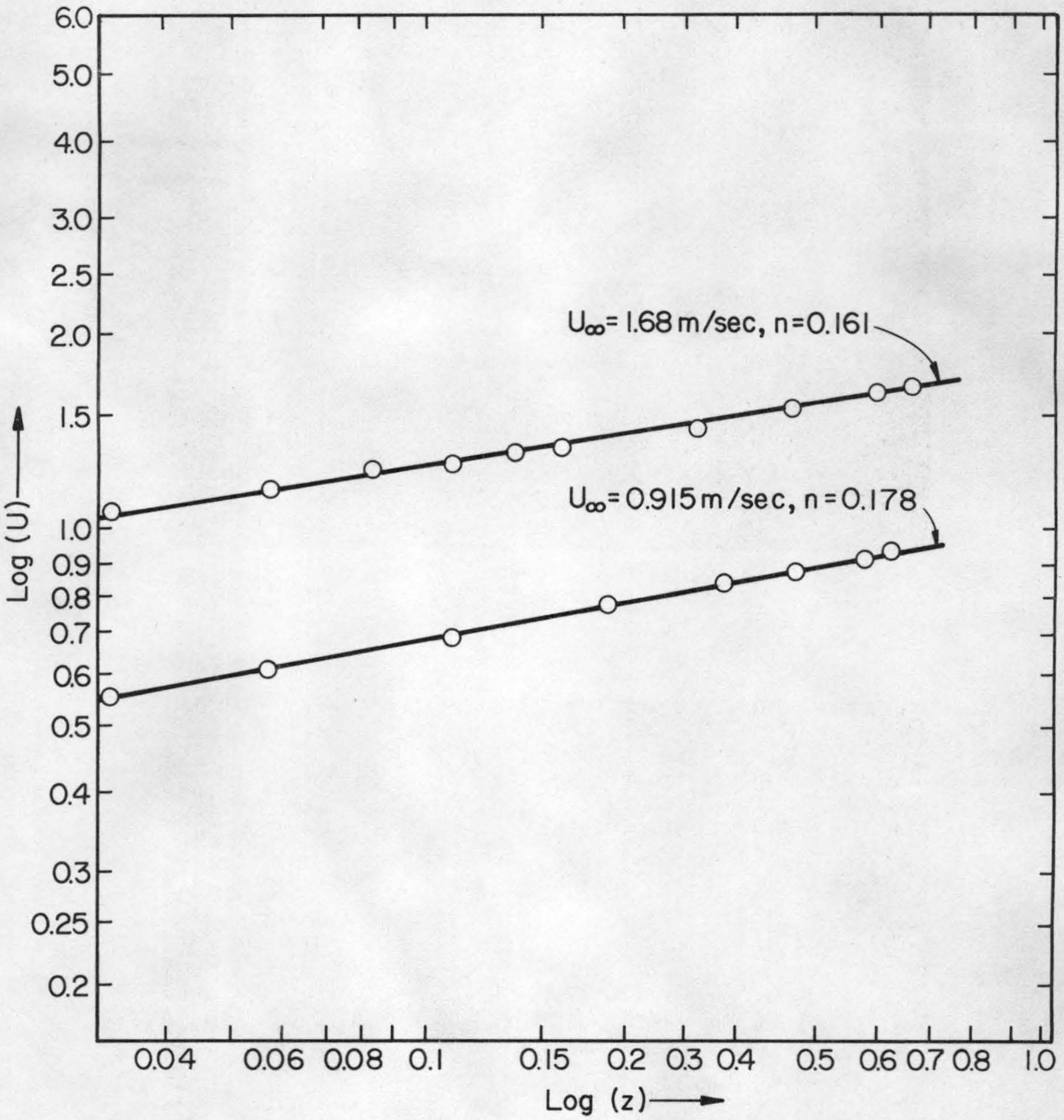

Fig. 9. Estimation of n of power law of velocity profiles.
$x = 9m \quad y = 0$.

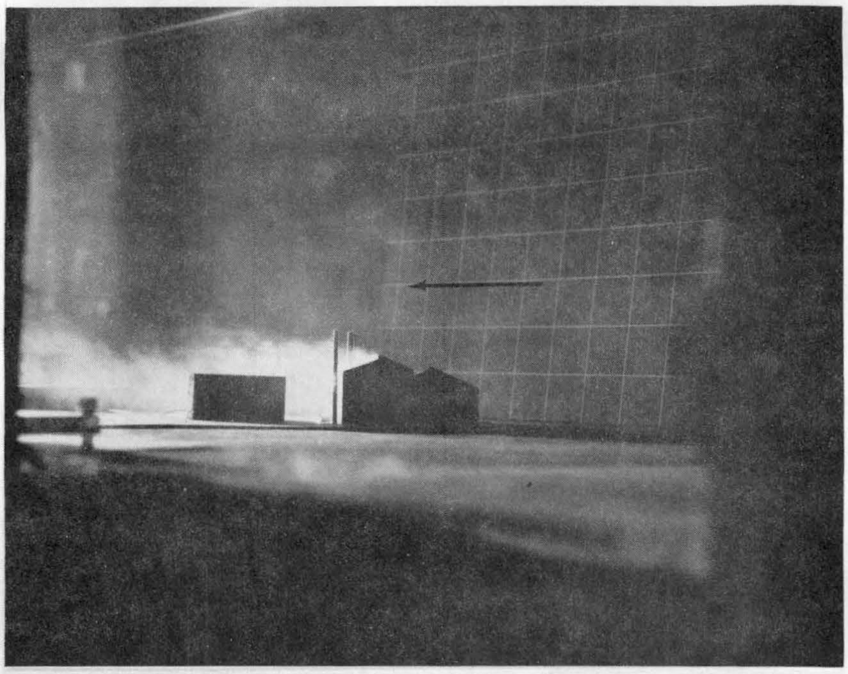

Fig. 10 Flow cavity downwind of the power-plant structure — flow visualization

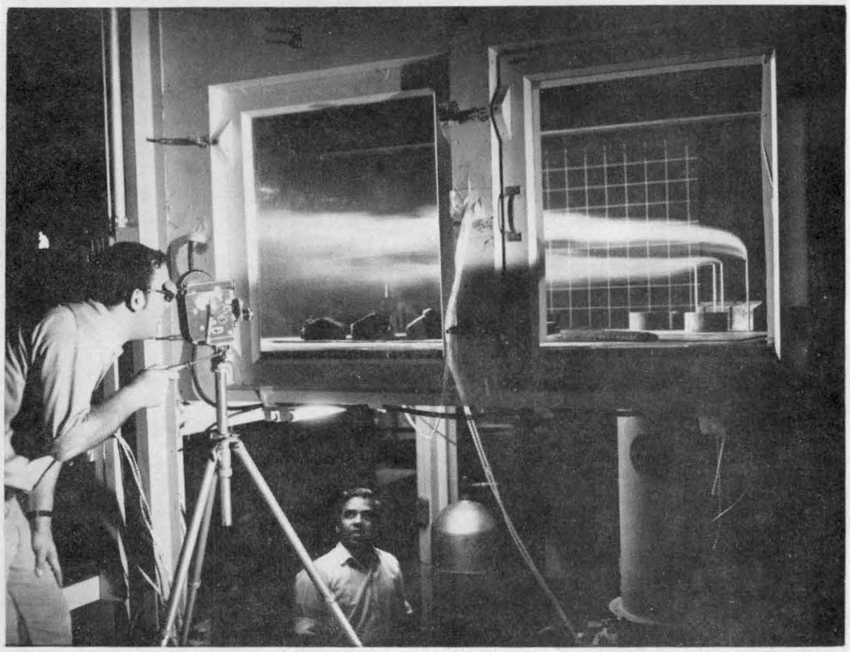

Fig. 11 Motion picture photography of plumes (stack height 53.34 m)

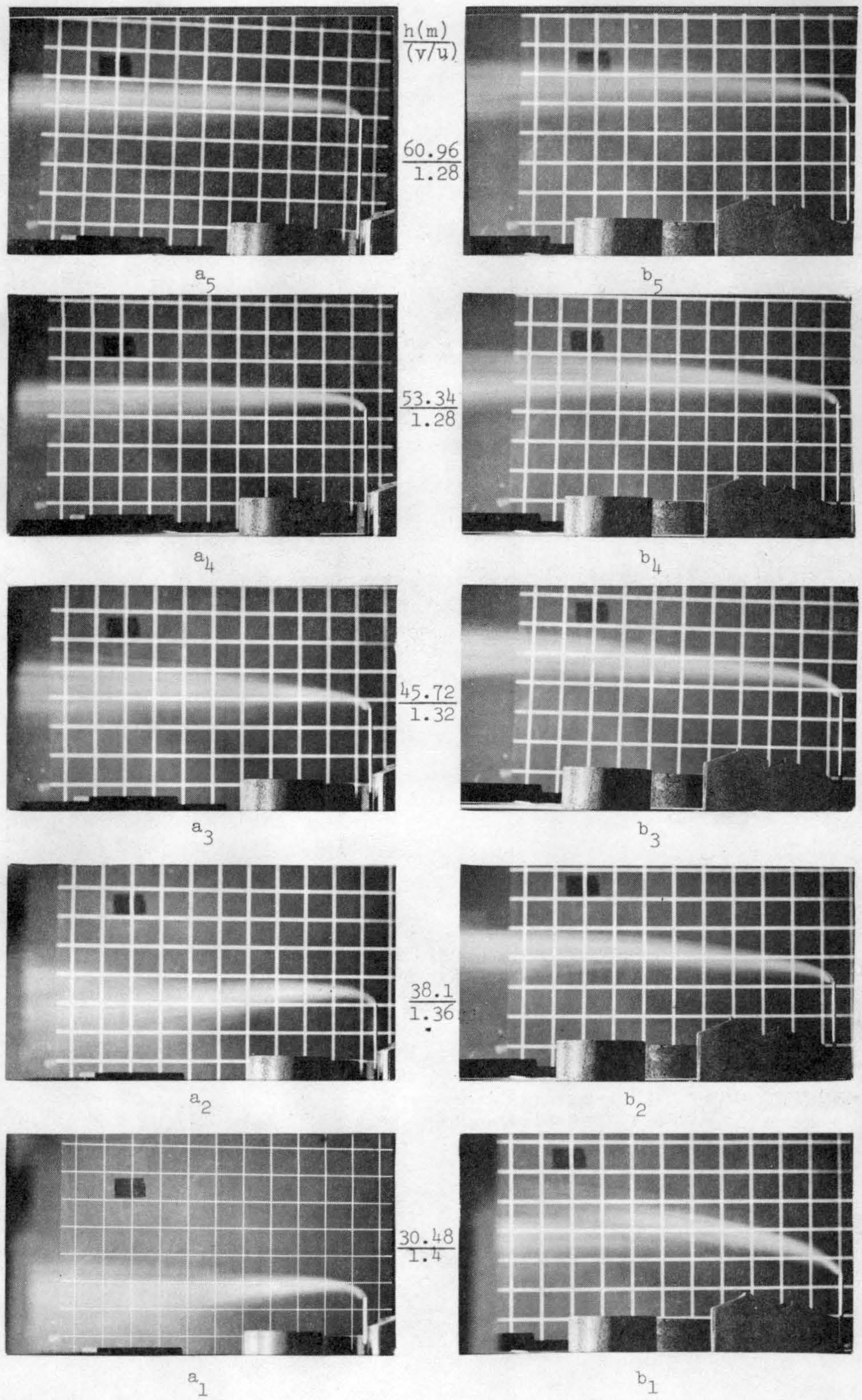

Fig. 12. Characteristics of exhaust plume for stacks located a) downwind, b) upwind of the power plant structure. Grid interval - 22 meters. Stack 3.

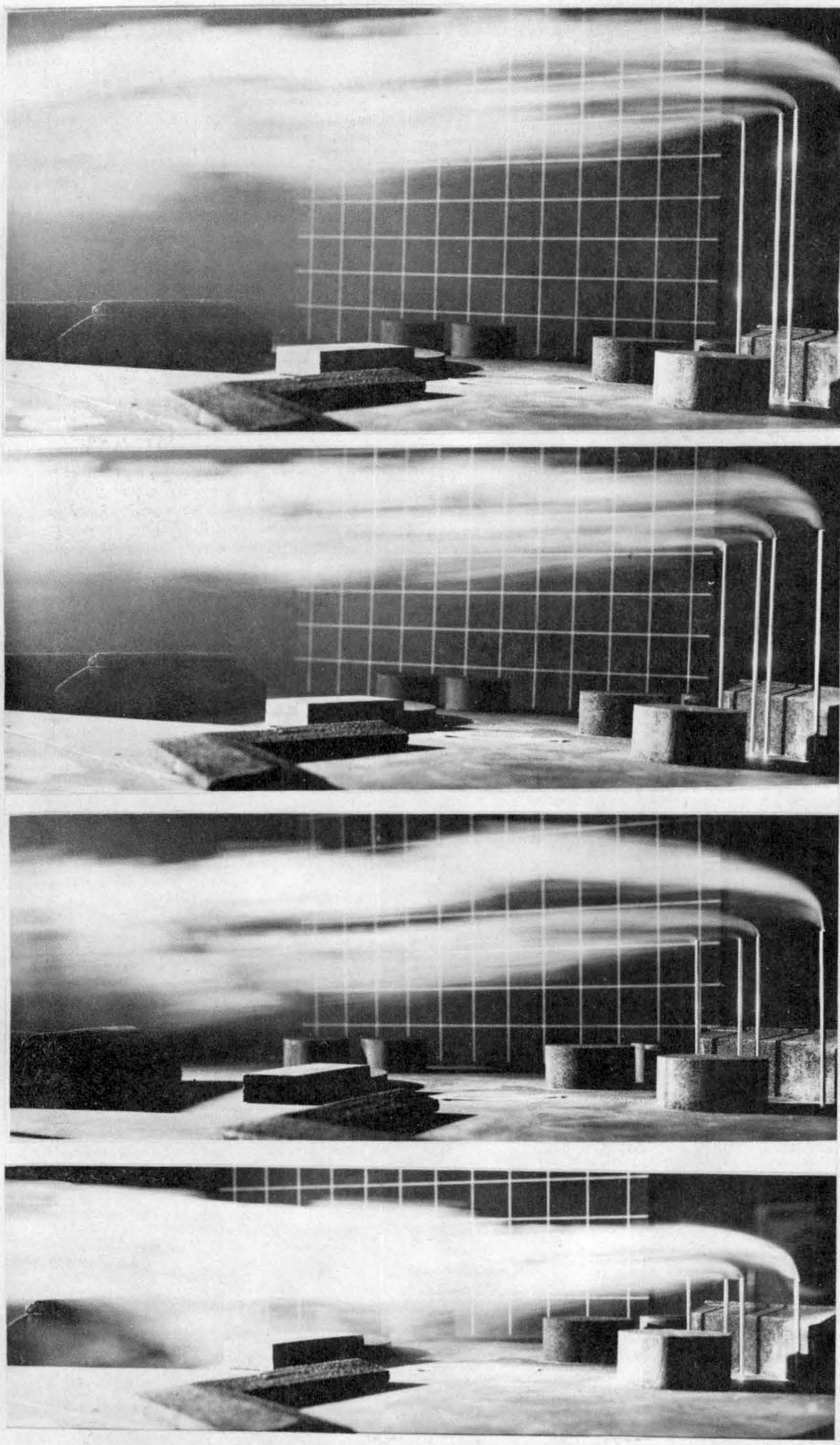

$h = 91.44$ m
$r_1 = 0.66$
$r_2 = 0.56$
$r_3 = 1.18$
$r_4 = 2.67$

$h = 60.36$ m
$r_1 = 0.71$
$r_2 = 0.60$
$r_3 = 1.26$
$4_4 = 2.85$

$h - 45.72$ m
$r_1 = 0.74$
$r_2 = 0.63$
$r_3 = 1.32$
$r_4 = 2.99$

$h = 30.48$ m
$r_1 = 0.79$
$r_2 = 0.67$
$r_3 = 1.40$
$r_4 = 3.19$

$U_\infty = 0.985$ m/sec, $n = 0.16$, $d = 6$ mm

Fig. 13 Flow visualization of exhaust plumes

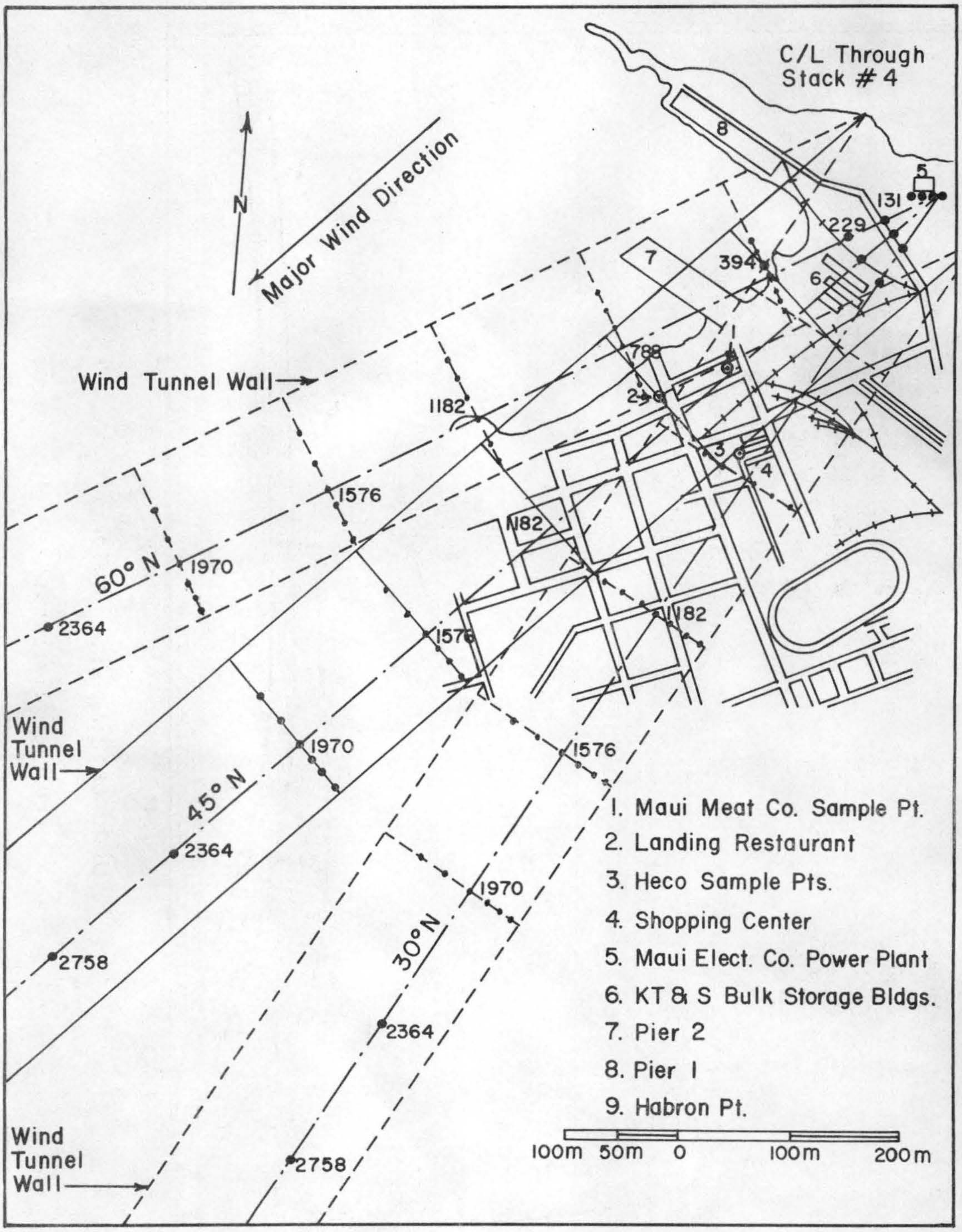

Fig. 14. Details of the area under investigation.

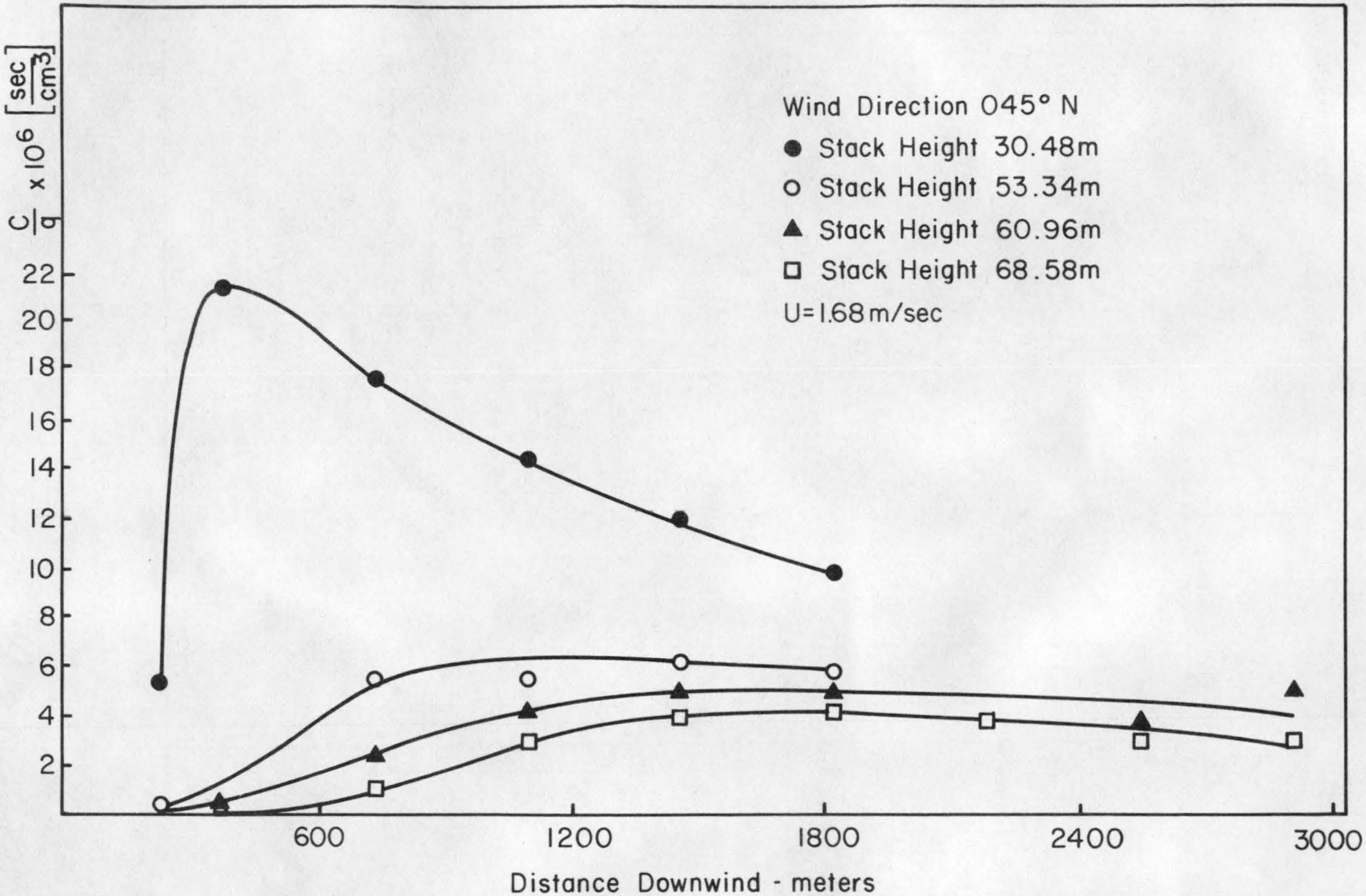

Fig. 15. Centerline ground-level concentration distribution. Wind direction: 045°N.-All stacks operational.

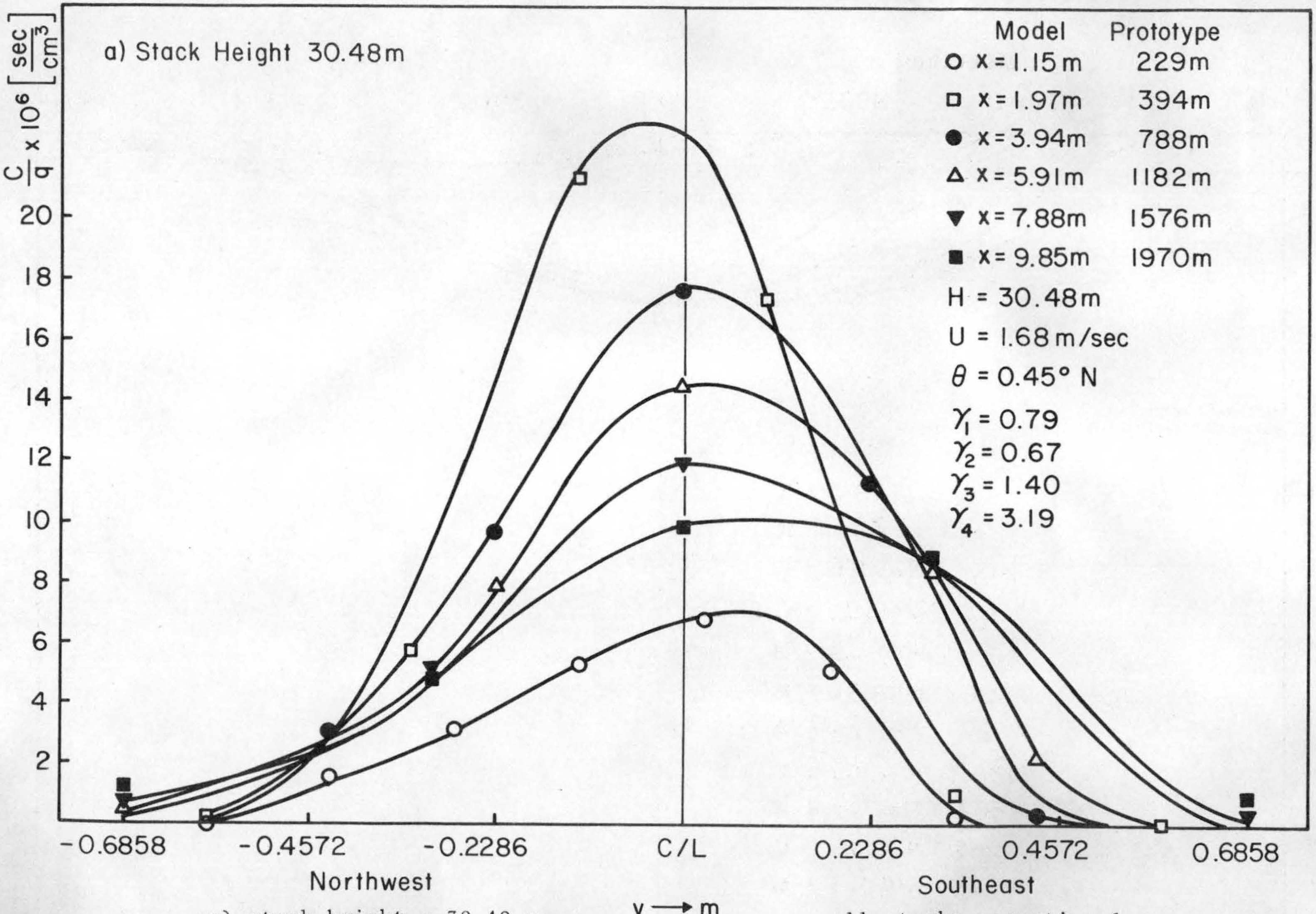

a) stack height = 30.48 m. -all stacks operational.

Fig. 16a. Sectional concentration distribution for wind 045°N.

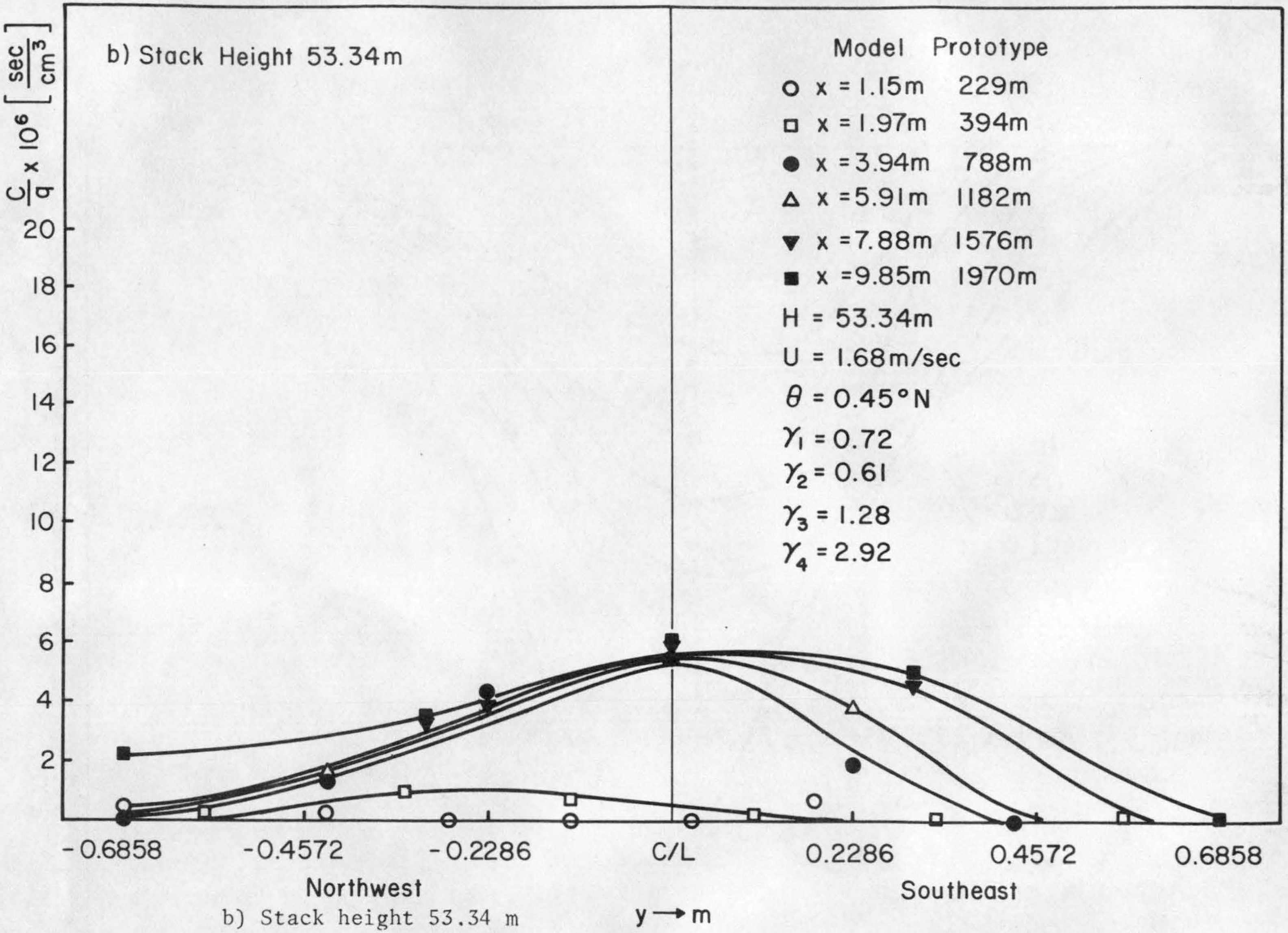

b) Stack height 53.34 m

Fig. 16b. Sectional concentration distribution for wind - 045°N.
All stacks operational.

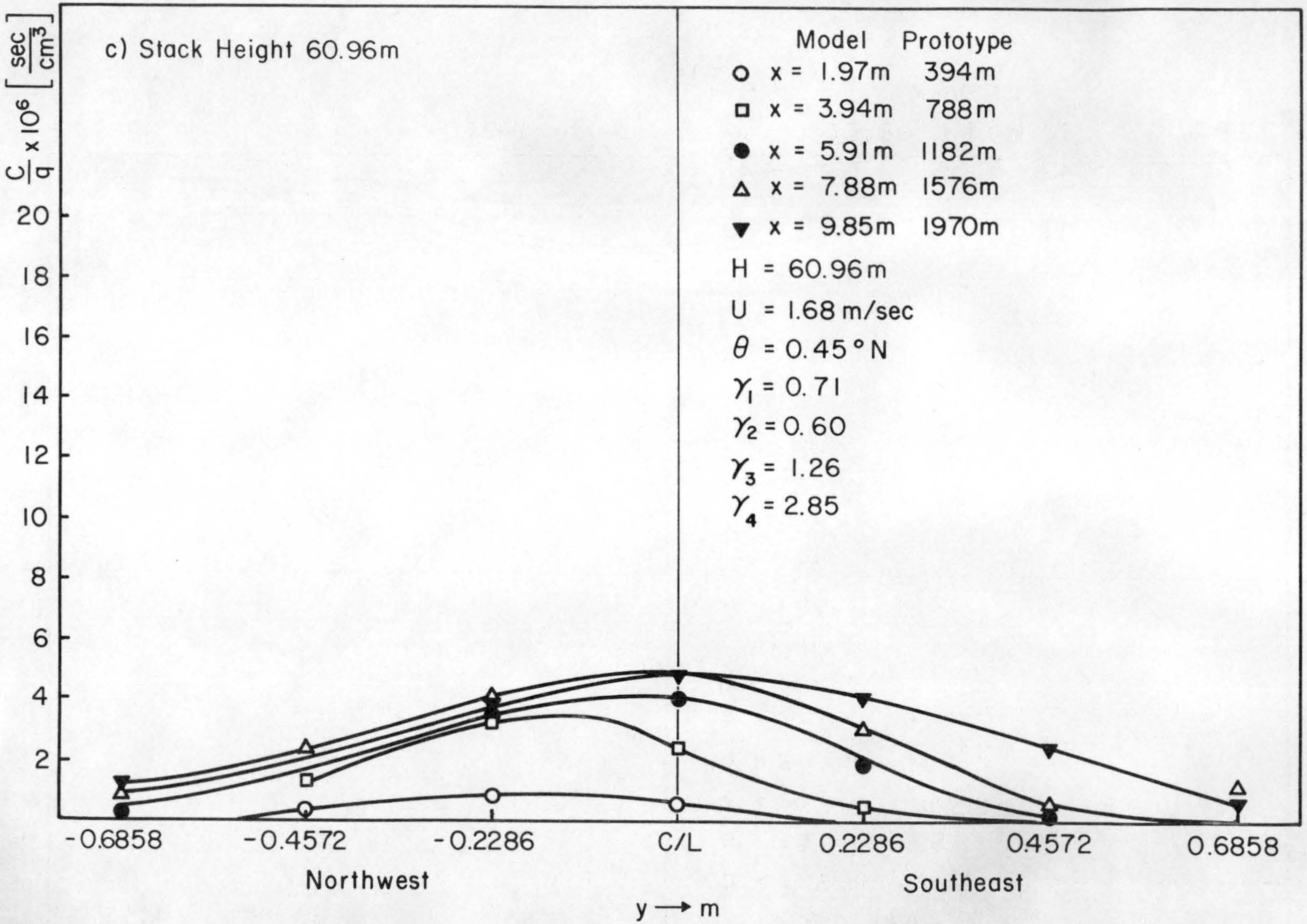

c) Stack height 60.96 m

Fig. 16c. Sectional concentration distribution for wind - 045°N.
All stacks operational.

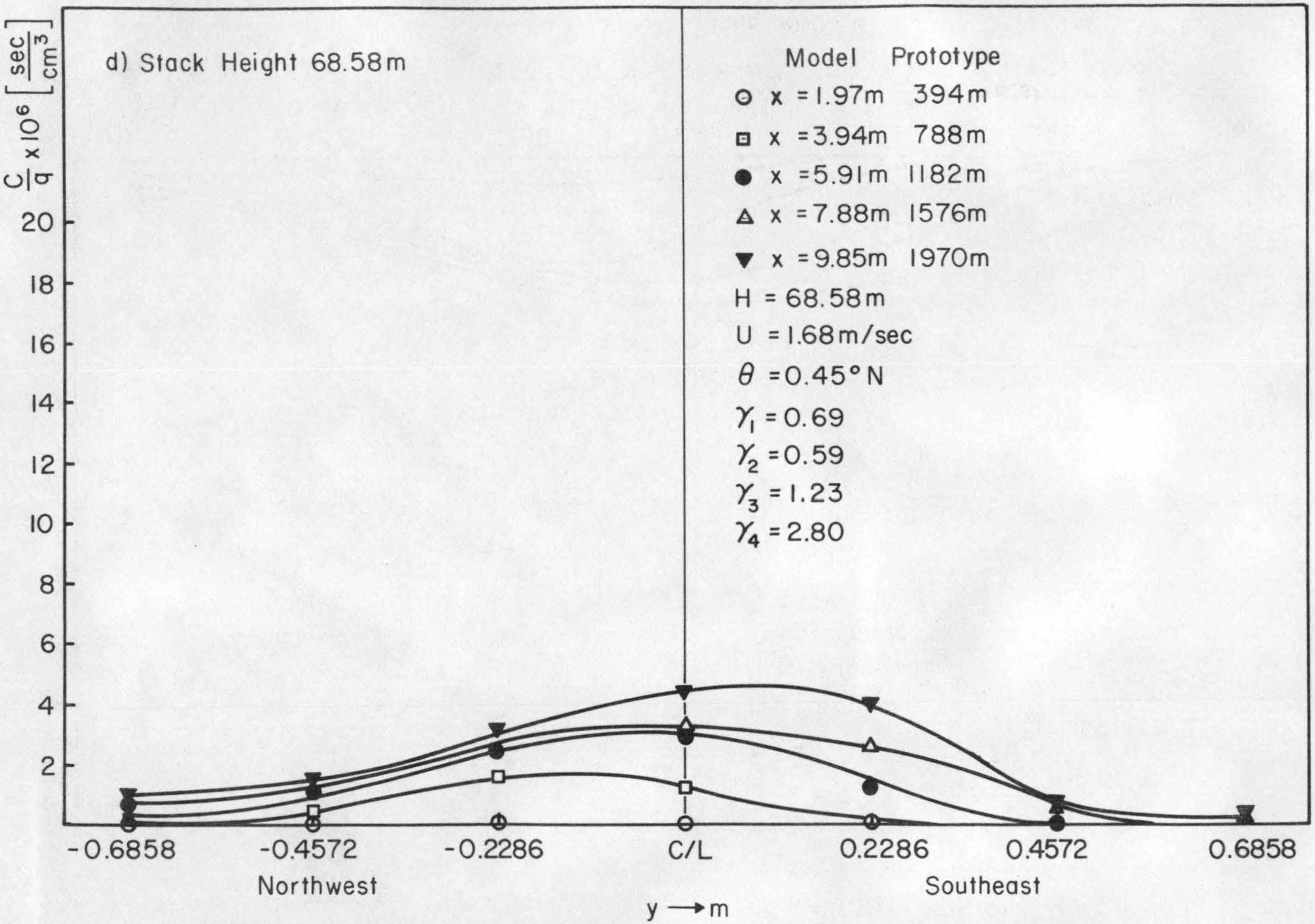

d) Stack height 68.58 m.

Fig. 16d. Sectional concentration distribution for wind 045°N. All stacks operational.

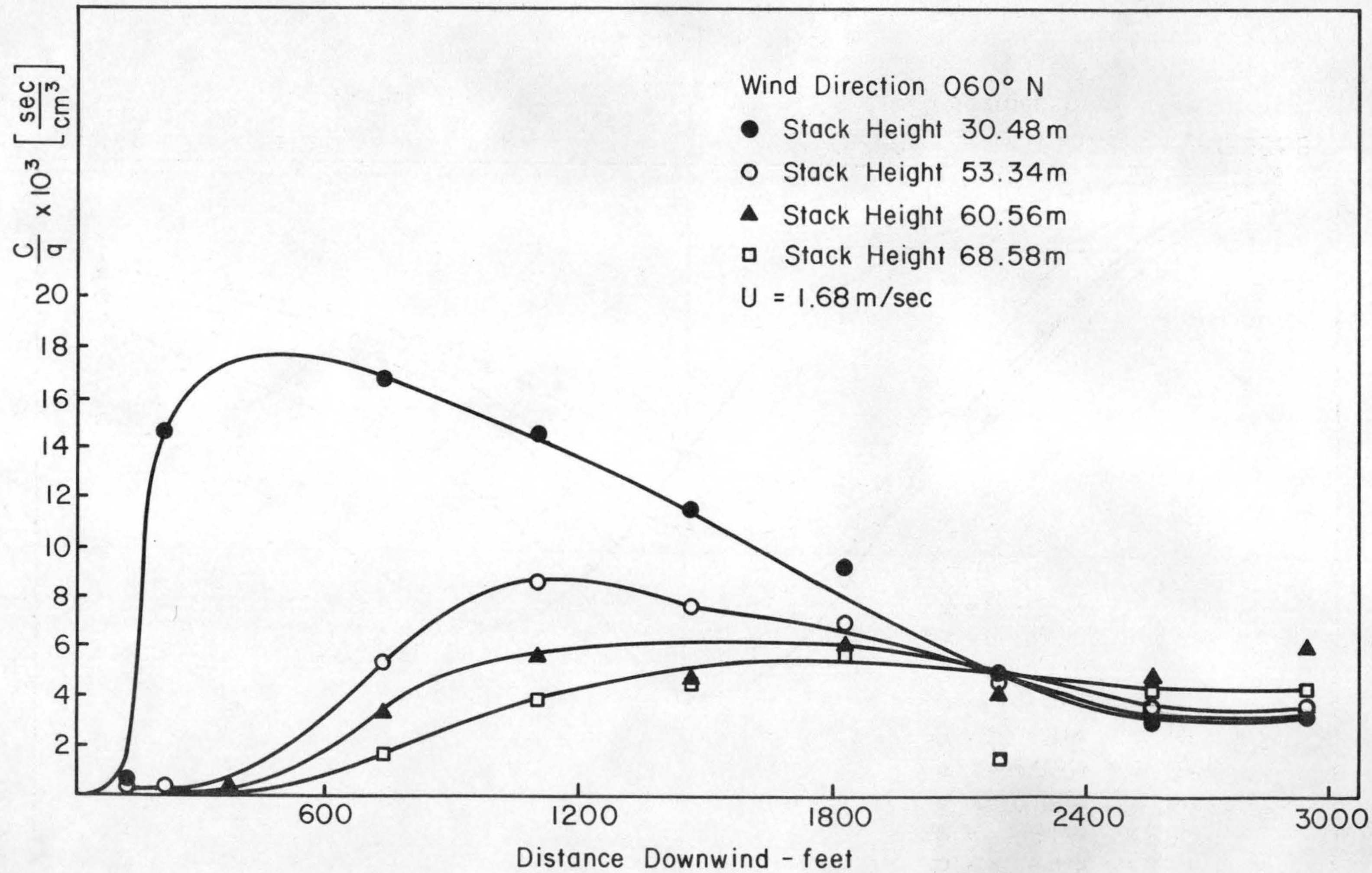

Fig. 17. Centerline concentration distribution for wind 060°N.
All stacks operational.

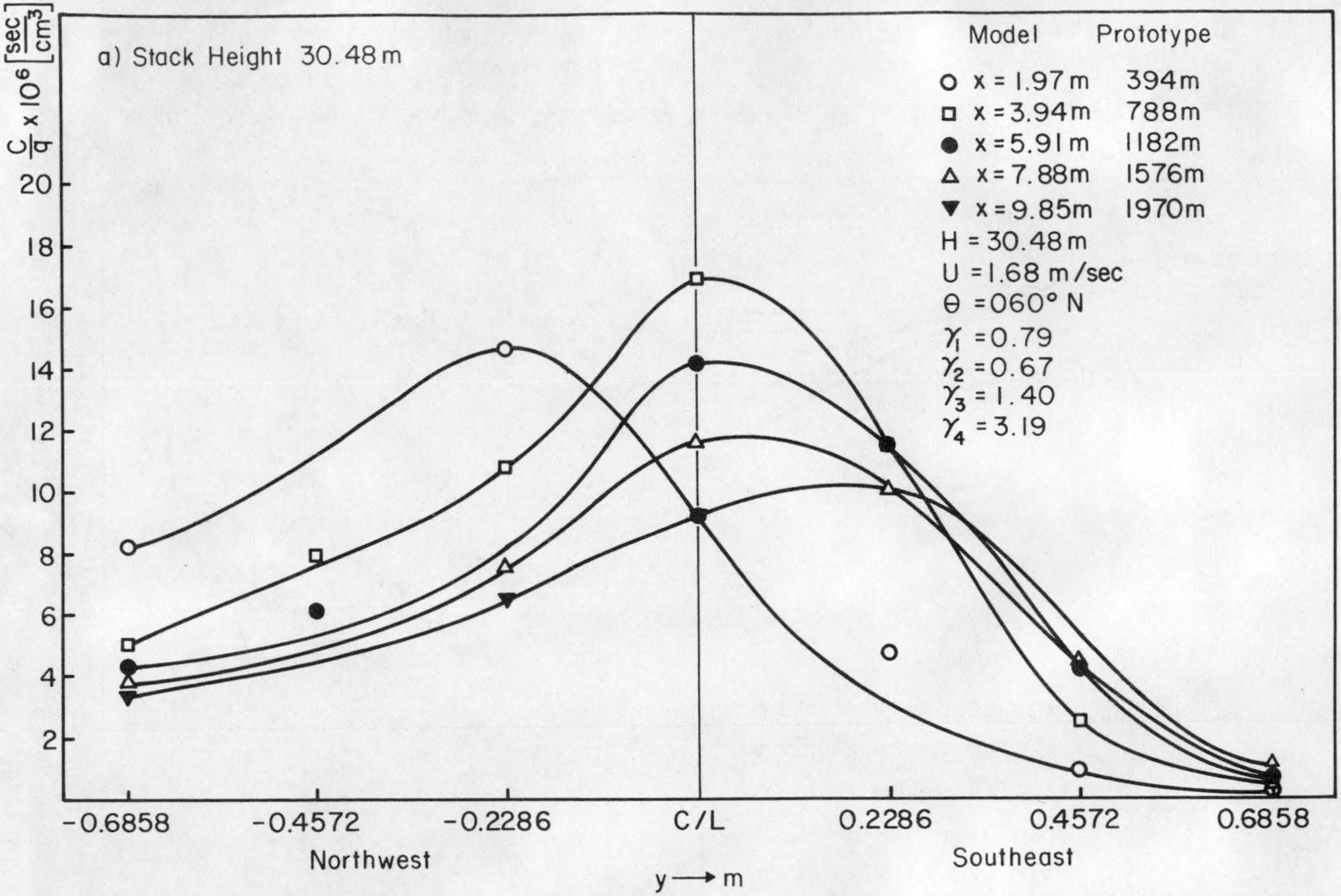

a) Stack height 30.48 m.

Fig. 18a. Sectional concentration distribution for wind - 060°N . All stacks operational.

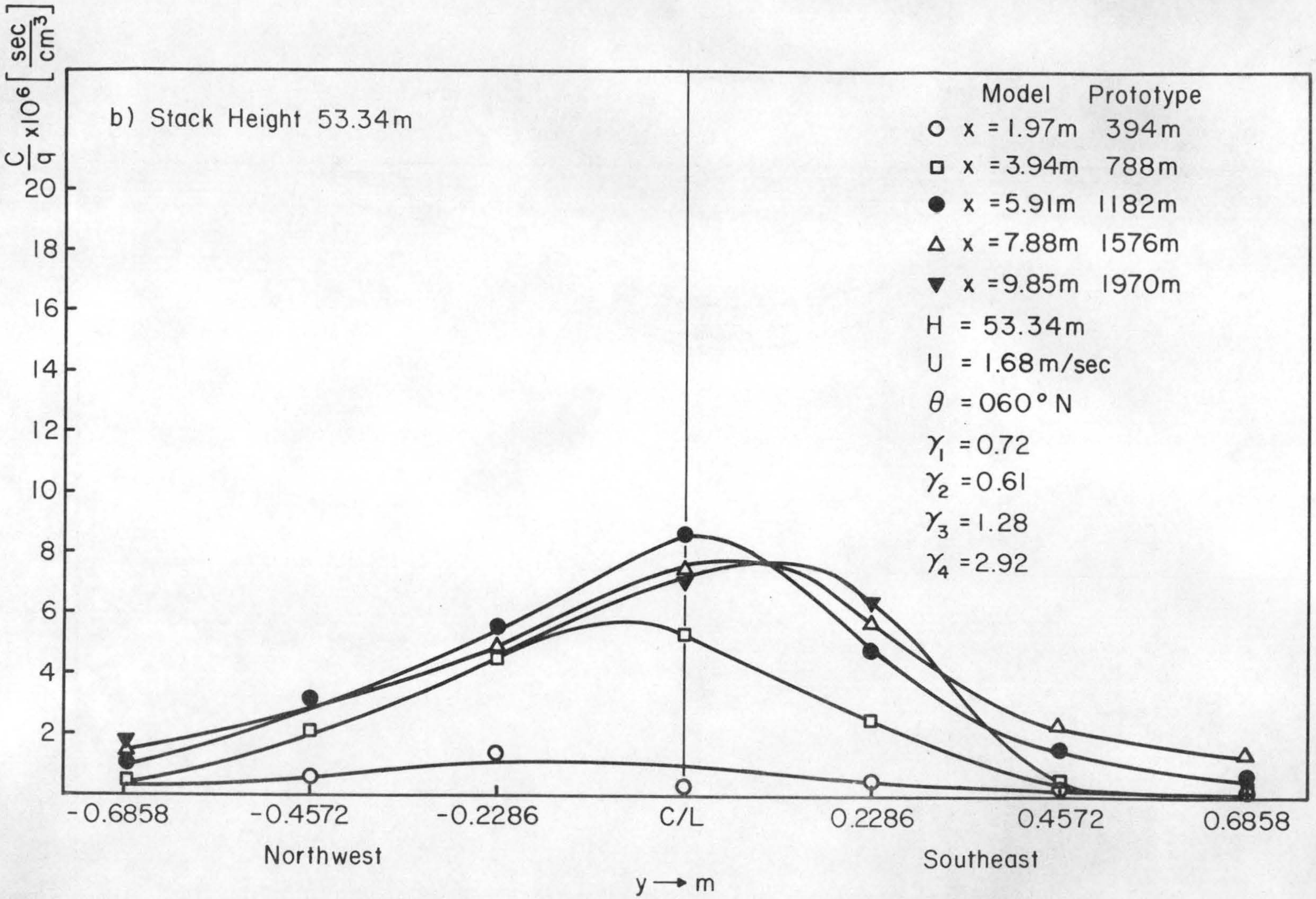

b) Stack height 53.34 m.

Fig. 18b. Sectional concentration distribution for wind - 060°N . All stacks operational.

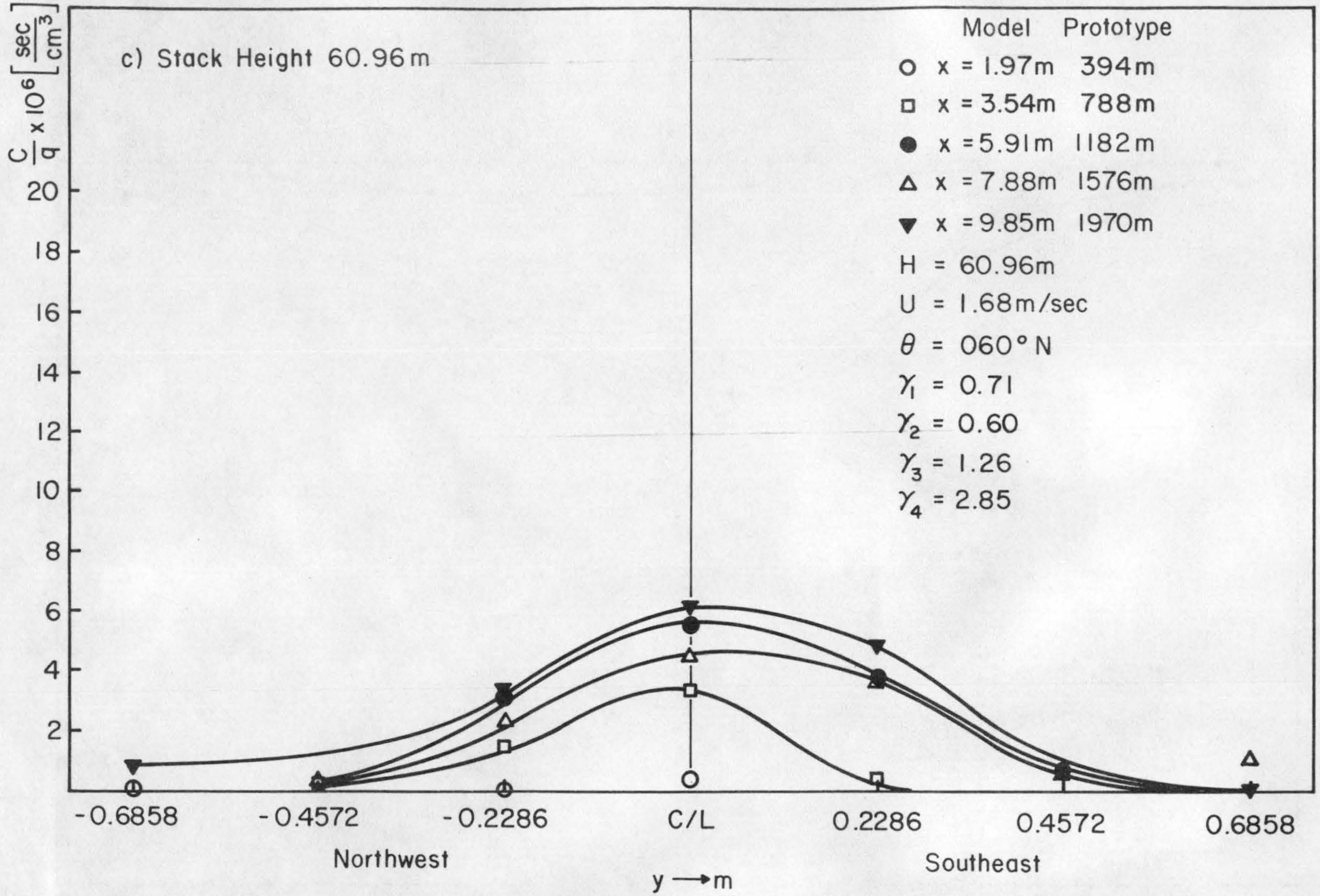

c) Stack height 60.96 m .

Fig. 18c. Sectional concentration distribution for wind - 060°N . All stacks operational.

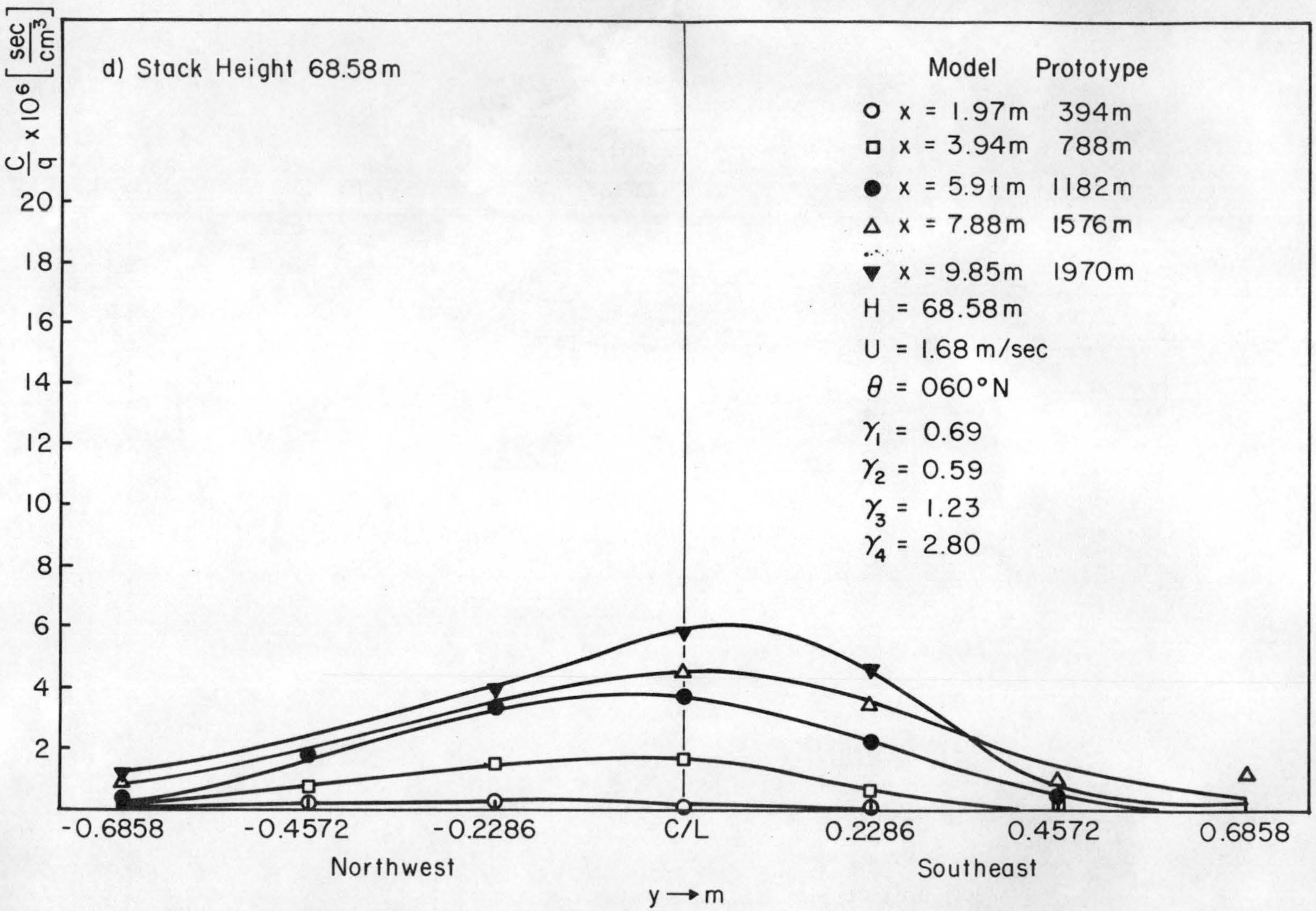

d) Stack height 68.58 m .

Fig. 18d. Sectional concentration distribution for wind 060°N. All stacks operational.

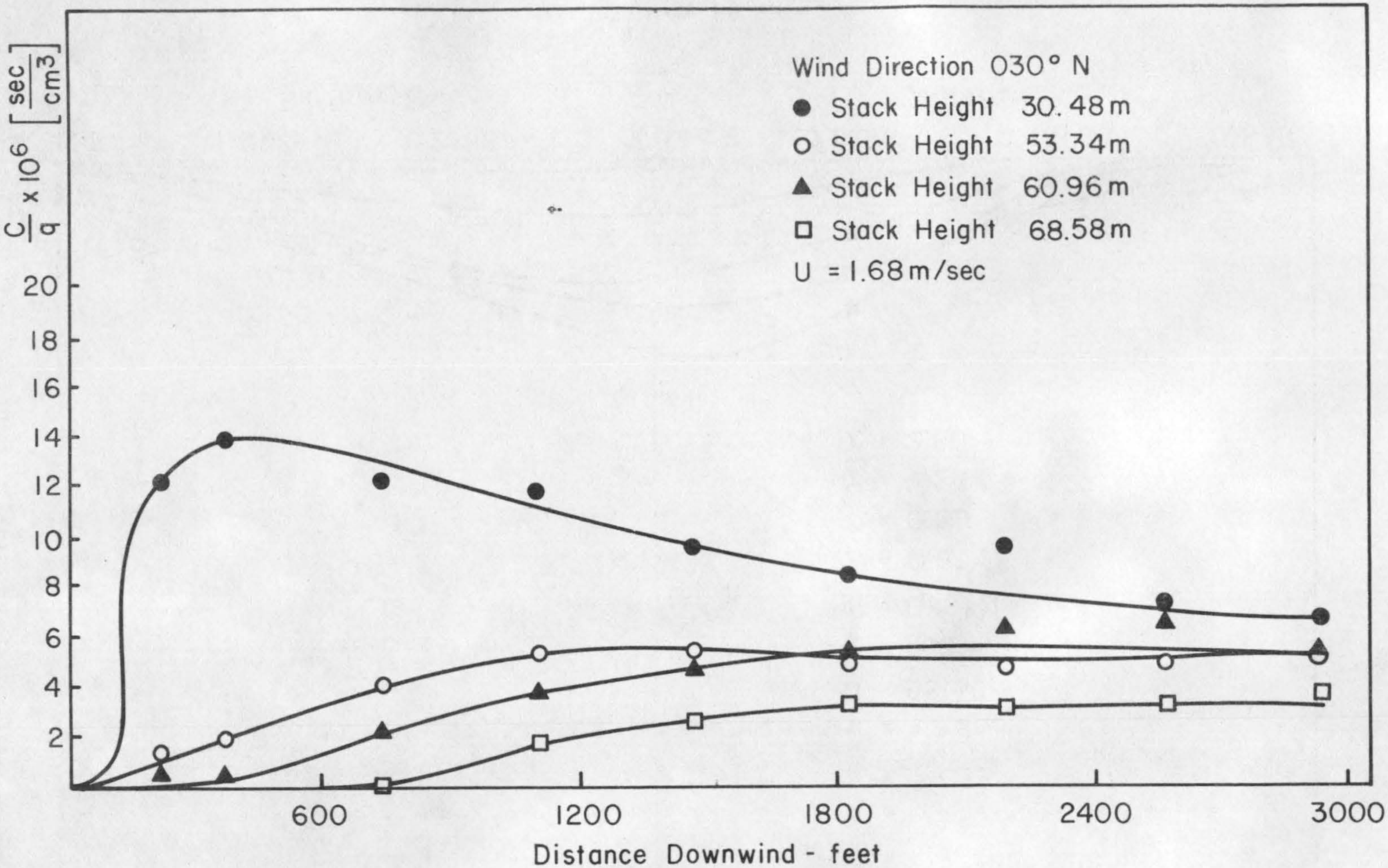

Fig. 19. Center line concentration distribution for wind 030°N , All stacks operational.

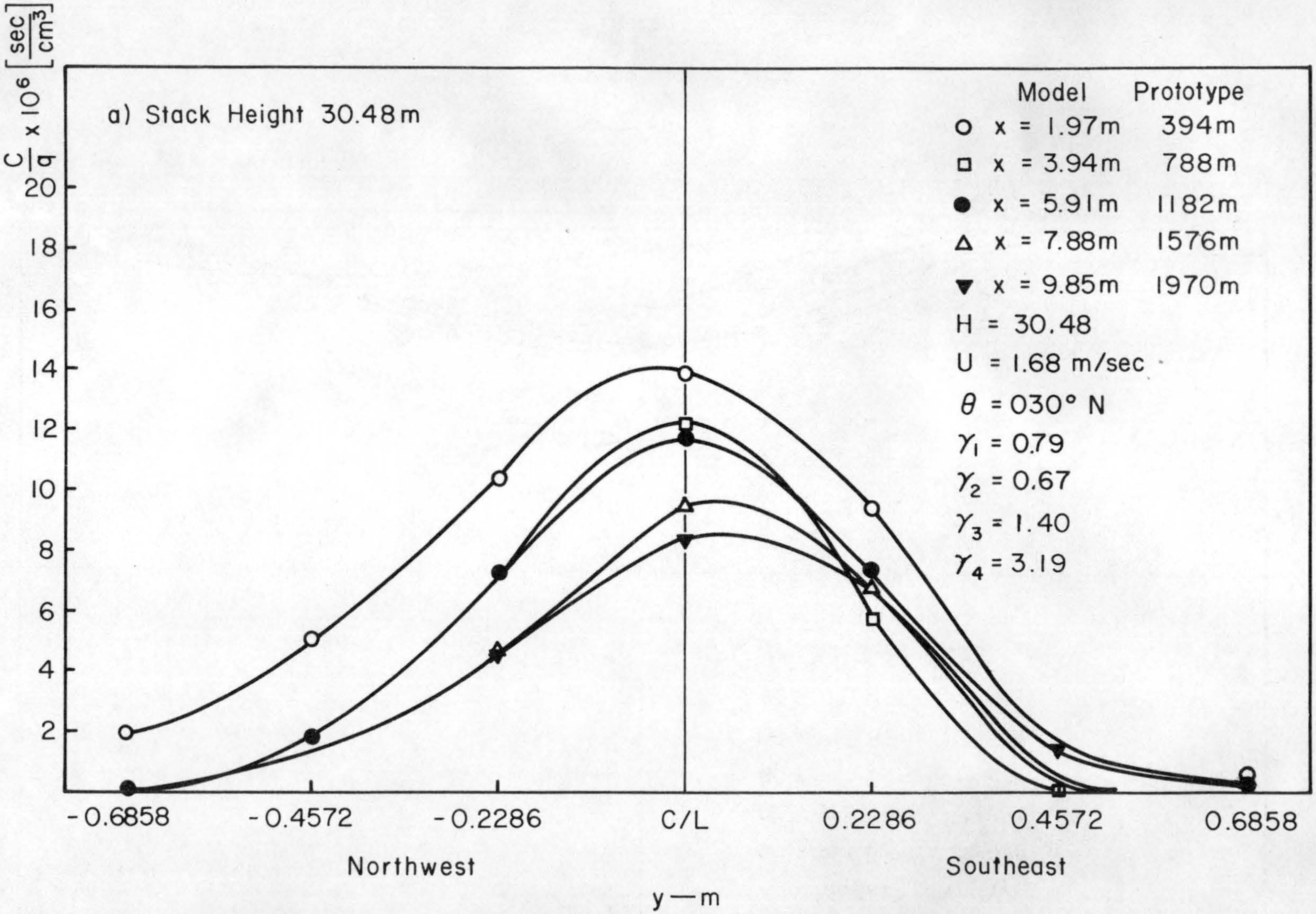

a) Stack height 30.48 m .

Fig. 20a. Sectional concentration distribution for wind direction 030° N , All stacks operational.

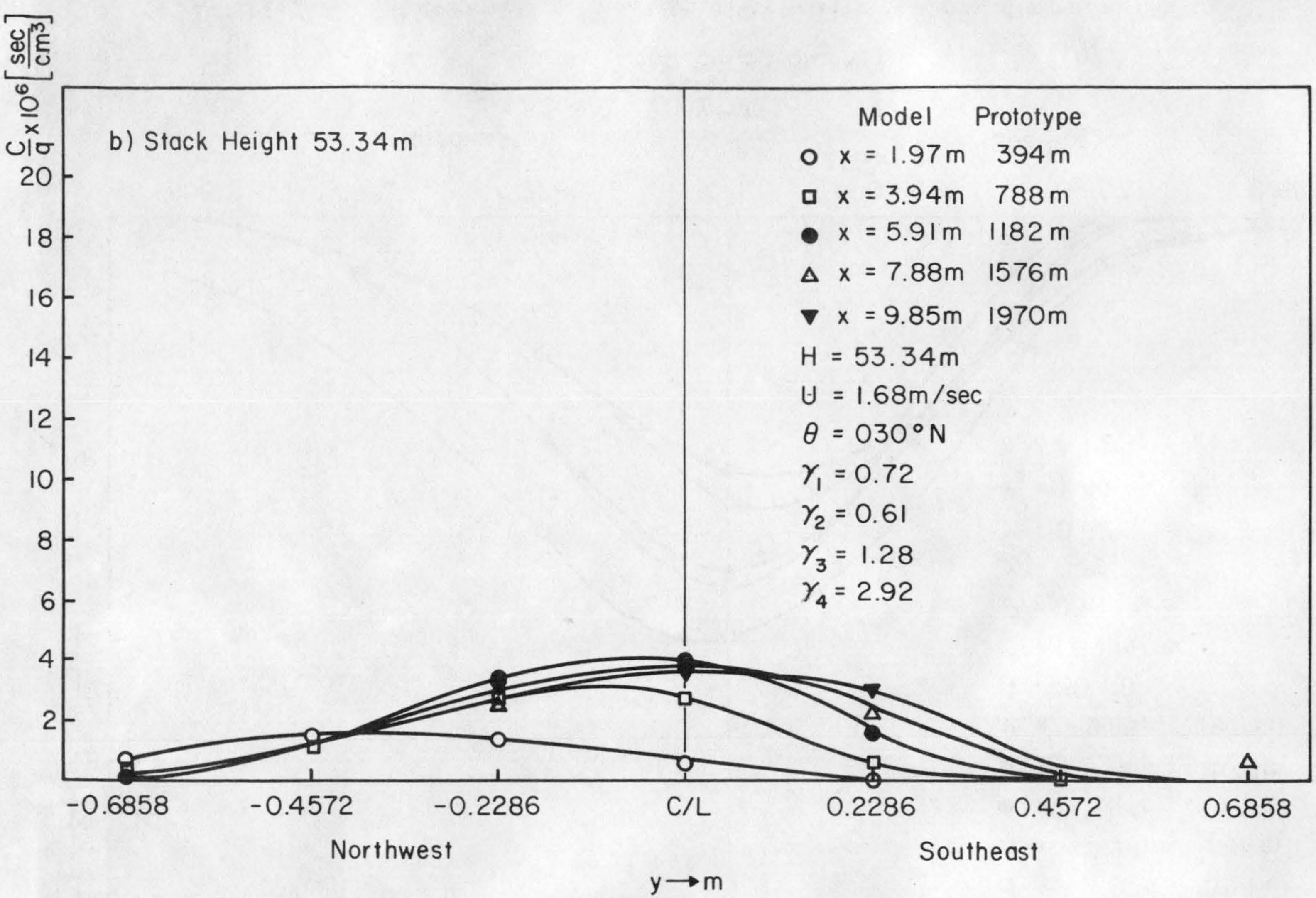

b) Stack height 53.34 m .

Fig. 20b. Sectional concentration distribution for wind direction 030° N . All stacks operational.

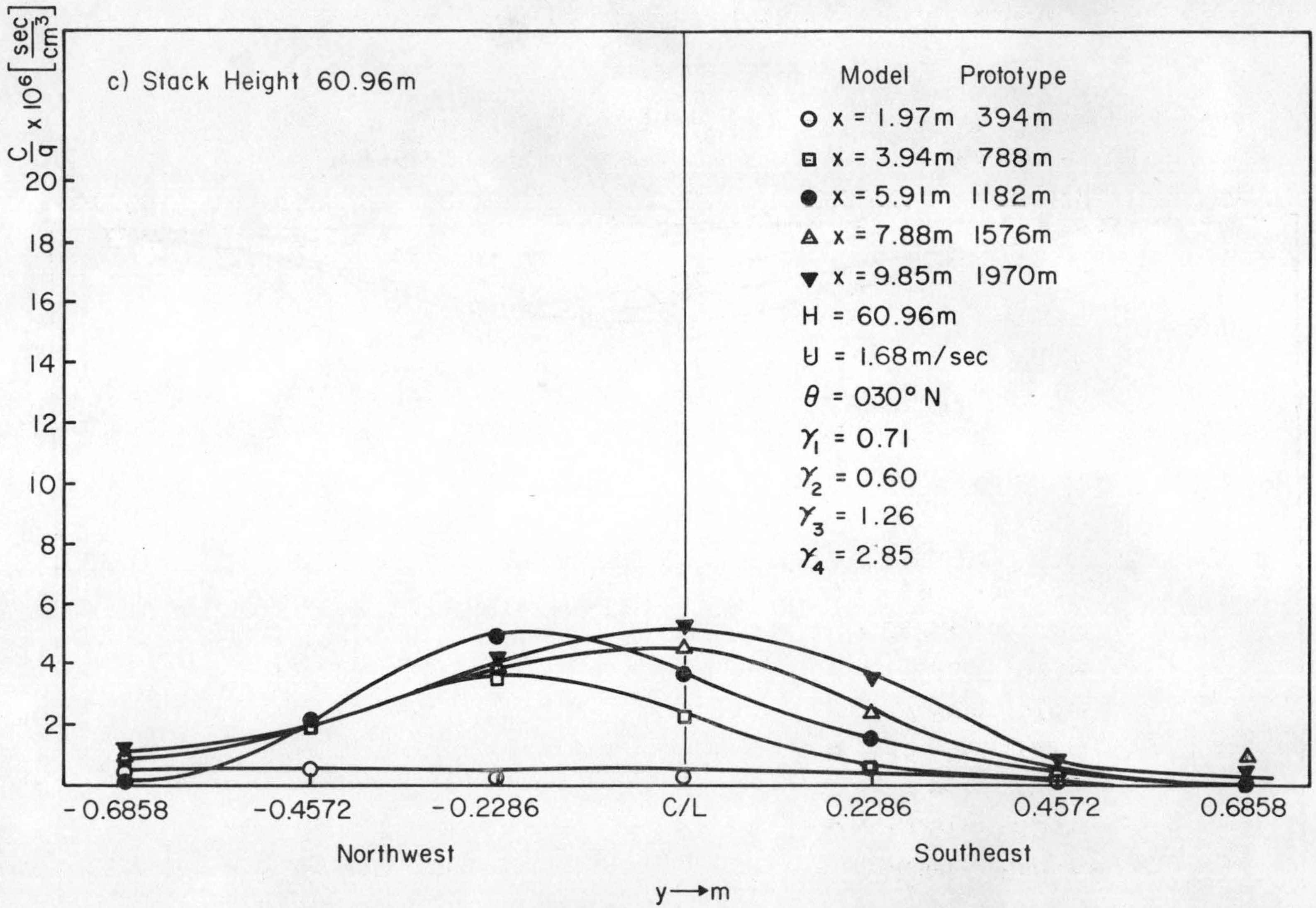

c) stack height 60.96 m.

Fig. 20c. Sectional concentration distribution for wind direction 030° N
All stacks operational.

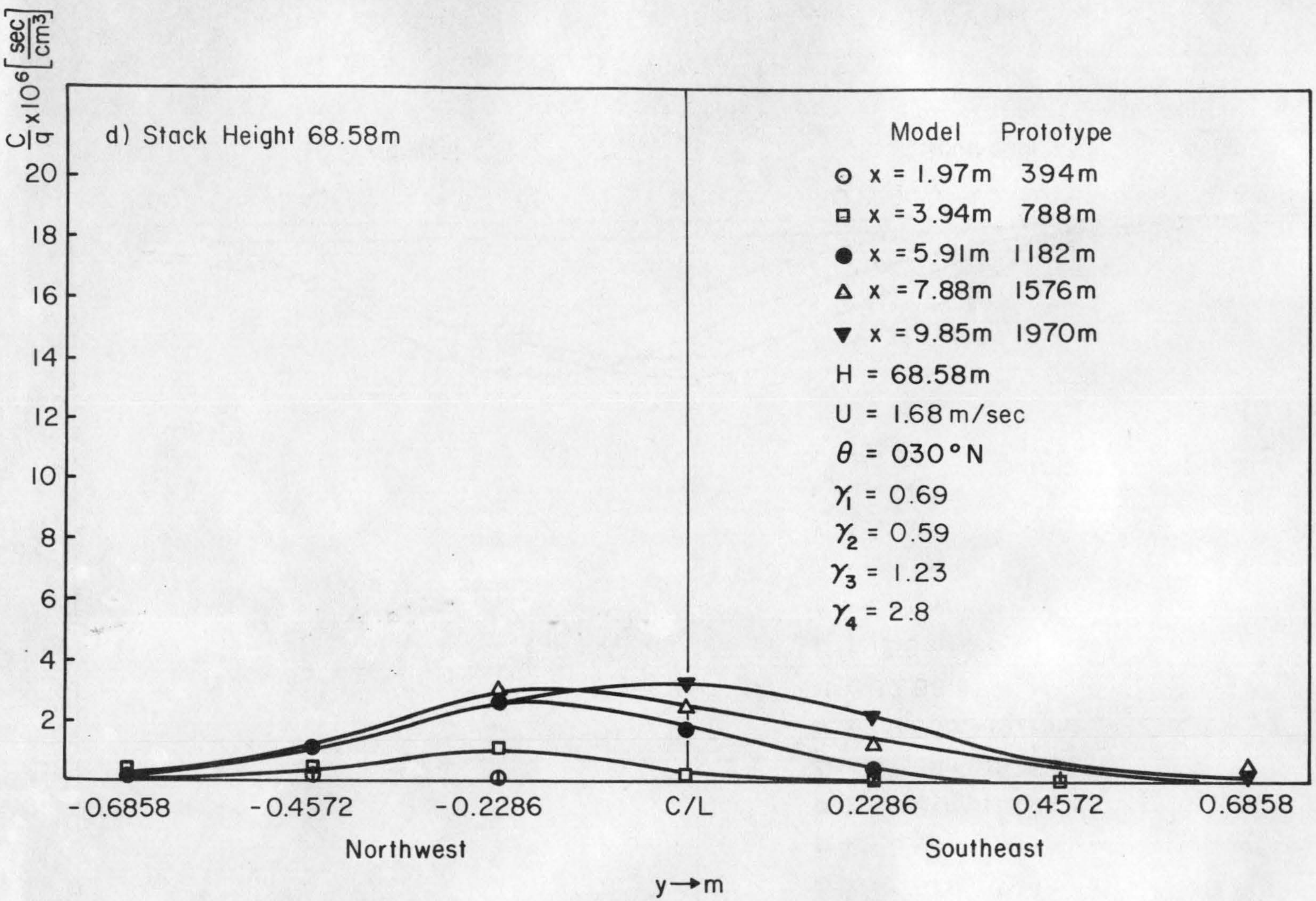

d) Stack height 68.58 m .

Fig. 20d. Sectional concentration distribution for wind direction 030° N .
All stacks operational.

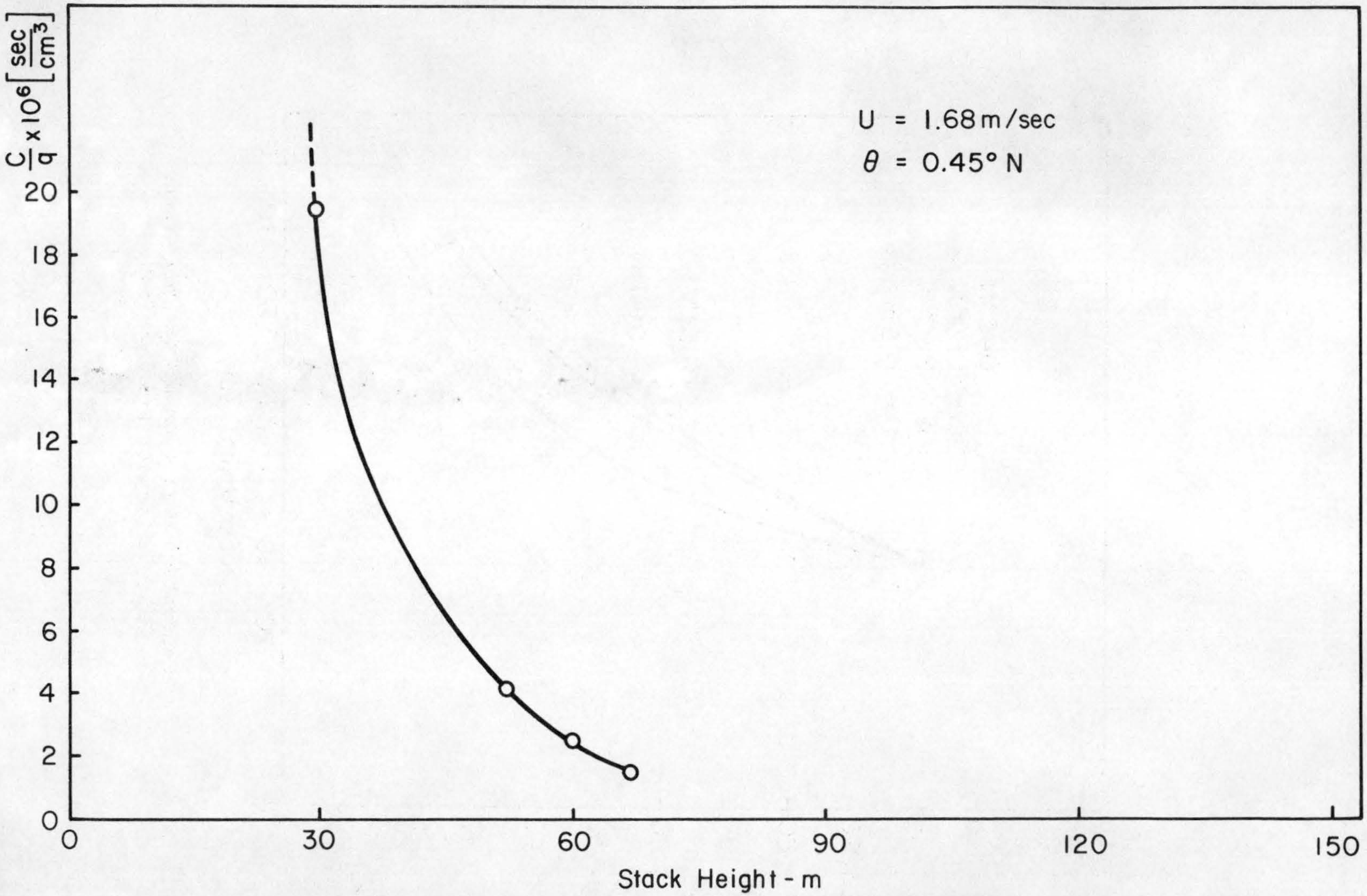

Fig. 21. Effect of stack height on concentration at Maui Meat Company. Wind:045°N
All stacks operational.

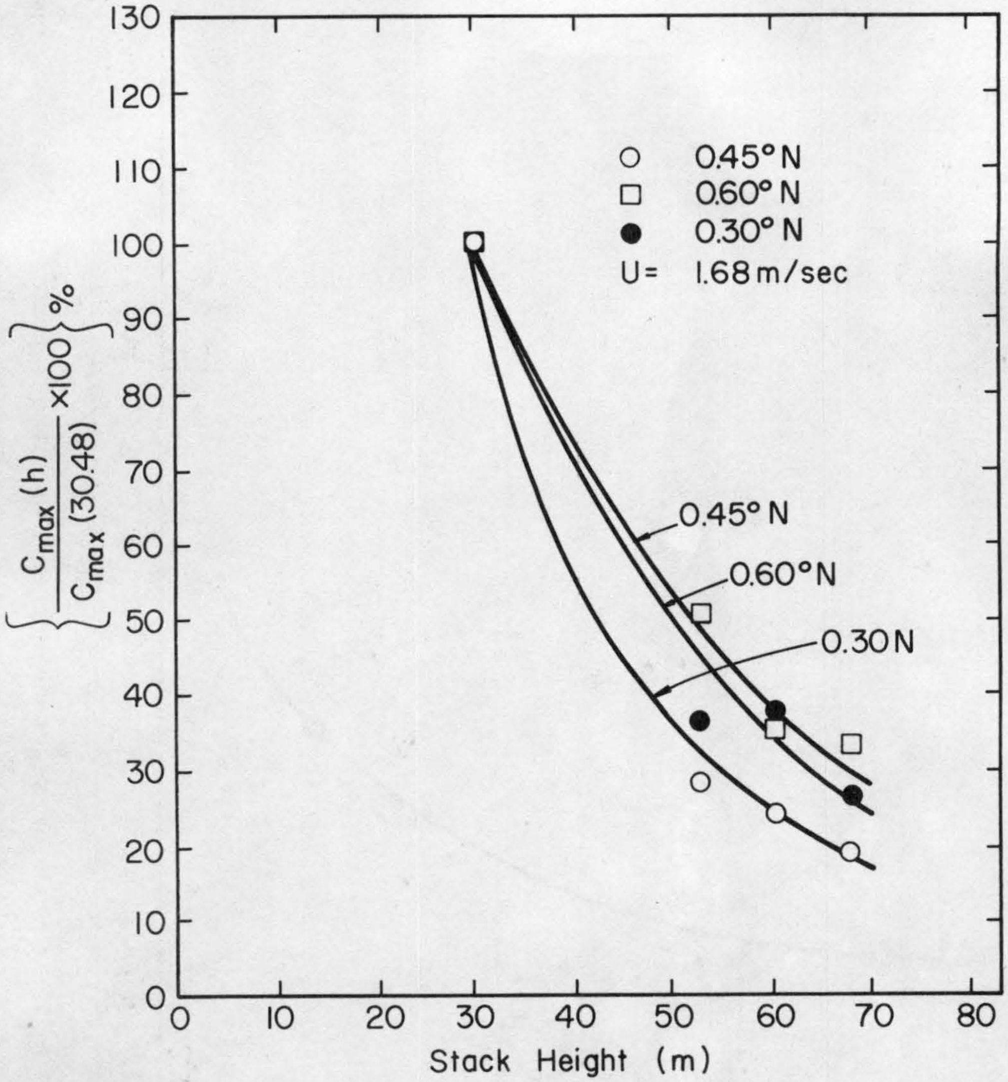

Fig. 22. Percentage variation of maximum ground-level concentration with stack height.

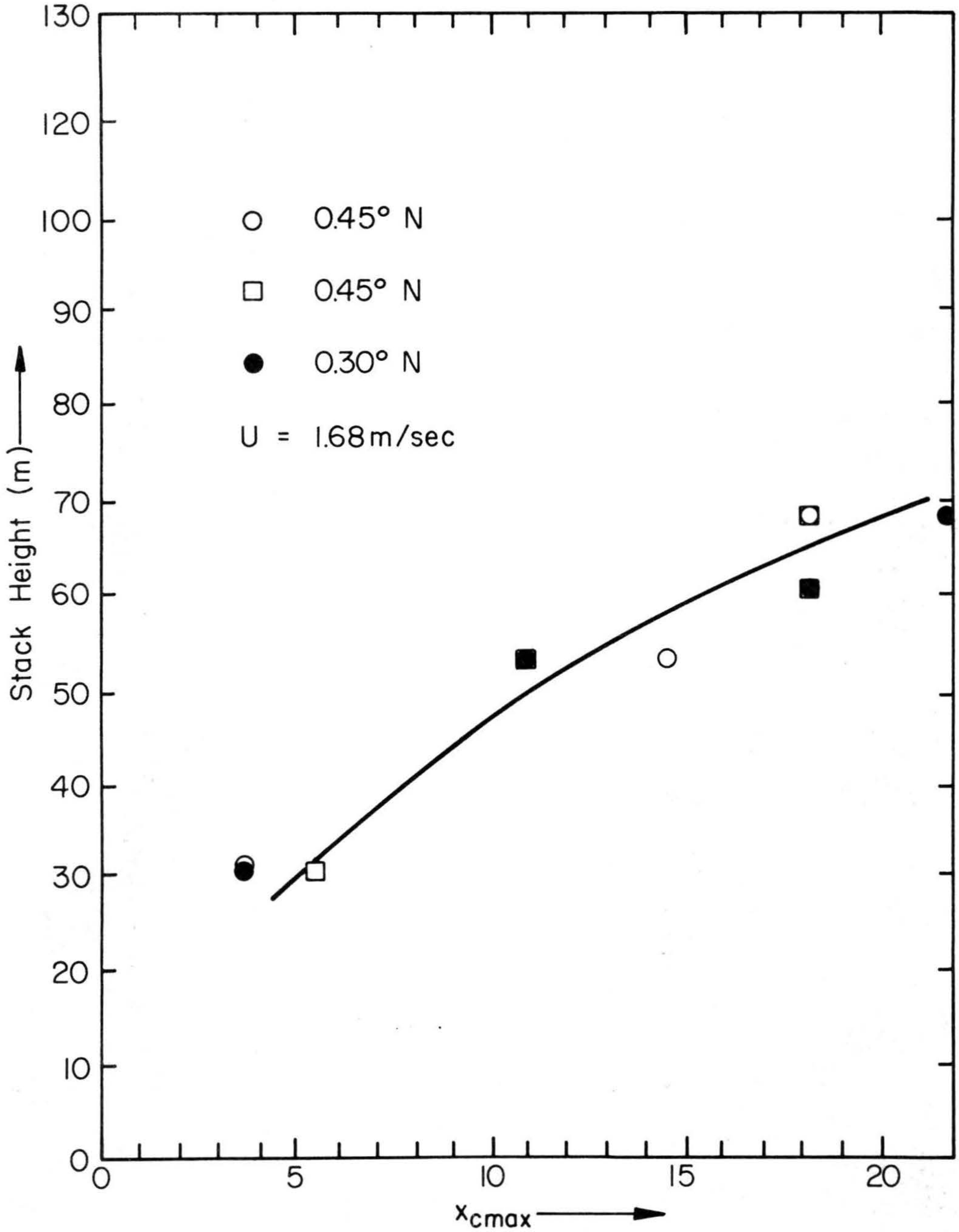

Fig. 23. Location of maximum ground-level concentration as a function of stack height.

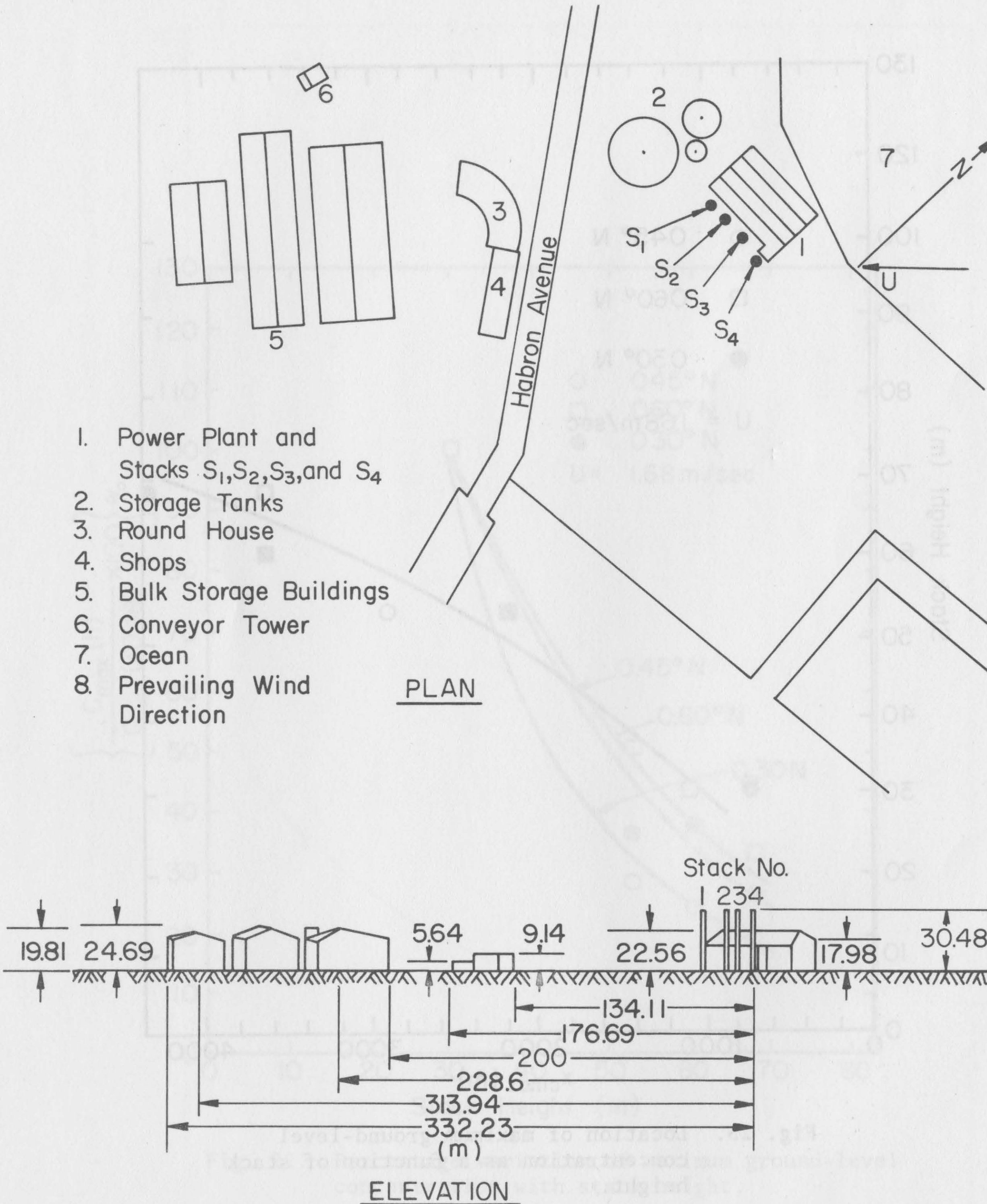

Fig. 24. Major Building details in the vicinity of Maui Electric Co. Power-Plant, Kahului, Maui, Hawaii.